THESIS FOR THE DEGREE OF DOCTOR OF PHILOSOPHY

HAM-Tools

An Integrated Simulation Tool for *H*eat, *A*ir and *M*oisture Transfer Analyses in Building Physics

ANGELA SASIC KALAGASIDIS

Department of Building Technology
Building Physics Division
CHALMERS UNIVERSITY OF TECHNOLOGY
Gothenburg, Sweden 2004

HAM-Tools
An integrated simulation tool for
*H*eat, *A*ir and *M*oisture transfer analyses in Building Physics
ANGELA SASIC KALAGASIDIS
ISBN 91-7291-439-4

Doktorsavhandlingar vid Chalmers tekniska högskola
Ny serie nr 2121
ISSN 0346-718x

Chalmers tekniska högskola
Institutionen för byggnadsteknologi, Byggnadsfysik
ISSN 1400-2728
P-04:1
Arbnr 985

Department of Building Technology, Building Physics Division
Chalmers University Of Technology
SE-412 96 Gothenburg
Sweden
Telephone +46 (0) 31-772 1000
www.chalmers.se

Chalmers Reproservice
Gothenburg, Sweden, 2004

HAM-Tools

An Integrated Simulation Tool for *H*eat, *A*ir and *M*oisture Transfer Analyses in Building Physics

ANGELA SASIC KALAGASIDIS
Department of Building Technology, Building Physics Division
Chalmers University of Technology

Abstract

'HAM-Tools' is a building simulation software. 'HAM' stands for *H*eat, *A*ir and *M*oisture transport processes in a building and building envelope that can be simulated by this program, and 'Tools' describes its modular structure. The main objective of this tool is to obtain simulations of transfer processes related to building physics, i.e. heat and mass transport in buildings and building components in operating conditions. The tool is to be used as a research and educational tool for the investigation of the mechanism of the above mentioned processes and of the degree of their correlation when they are coupled.

Using the graphical programming language Simulink®, the code is developed as a library of predefined calculation procedures (tools) where each supports the calculation of the HAM transfer processes in a building part or an interacting system. Tools are grouped according to their functionality into five sub-systems: Constructions (building envelope parts), Zones (air volume of the room), Systems (HVAC systems), Helpers (weather data) and Gains (casual gains). When all sub-systems are coupled together and solved simultaneously, the resulted simulation represents the highest level of integration in the HAM-Tools. The modular structure in Simulink, using systems and subsystems and the graphical approach, facilitate handling and control of a very complex interaction between different parts of the model.

This thesis encloses a presentation of HAM-Tools structure, mathematical and numerical models that it is based on, selected examples of the application of the code and results of validation tests.

As a part of the International Building Physics Toolbox, HAM-Tools is an open research tool and publicly available for a free downloading. Any researcher can use, expand and develop the contents of the library.

Keywords: HAM transfer, Whole building HAM model, International Building Physics Toolbox, Simulink modeling

The thesis consists of introductory summary and research articles, which will be referred to in the summary as **Paper I** to **Paper V**.

I. **Weitzmann, P., Sasic Kalagasidis, A., Nielsen, T.R., Peuhkuri, R., Hagentoft, C-E.** Presentation of the International Building Physics Toolbox for Simulink. *Proceedings of the 8th International Building Performance Simulation (IBPSA) Conference 2003.* Eindhoven, the Netherlands.

II. **Hagentoft C-E., Sasic Kalagasidis, A., Adl-Zarrabi, B.** Benchmarks for One-dimensional Cases of Combined Heat, Air and Moisture Transport in Building Components. *Proceedings of the CIB World Building Congress 2004.* Toronto, Canada.

III. **Sasic Kalagasidis, A., Hagentoft C-E.** The influence of air transport in and around the building envelope on energy efficiency of the building. *Research in Building Physics. Proceedings of the 2nd International Conference on Building Physics. 2003.* Leuven, Belgium.

IV. **Sasic Kalagasidis, A., Bednar, T., Hagentoft, C-E.** The evaluation of the interface moisture conductivity between control volumes. Comparison between linear, harmonic and integral averaging. *Submitted to the 9th International Conference on Performance of the Exterior Envelopes of Whole Buildings. 2004.* Clearwater Beach, Florida.

V. **Sasic Kalagasidis, A.** The whole model validation for HAM-Tools. Case study: hygro-thermal conditions in the cold attic under different ventilation regimes. *Submitted to the 9th International Conference on Performance of the Exterior Envelopes of Whole Buildings. 2004.* Clearwater Beach, Florida.

Acknowledgments

I hope that this work can express the joy I have had working for the past three years at the department, and also my passion towards the profession itself. There are people and institutions who helped me to succeed and feel so special about it. I would like to name them here and give my sincere gratitude.

This work is financially supported by the Swedish Research Council for Environment, Agricultural Science and Spatial Planning (FORMAS) through the project 'Air transport in and through the building envelope', and by Chalmers University of Technology. Both institutions are greatly acknowledged. Their grants provided the necessary environment for my everyday struggle.

I would like to express my special gratitude to Professor Carl-Eric Hagentoft, my thesis mentor, for all the confidence he has had in my work. After having started as a guest researcher in 2001, I continued the work he had initiated on developing Building Physics Toolbox. With his steady, trusty and patient support, it has been my privilege to work with him. I have also earned a lot of experience working with other national and international experts in building physics areas, which gave me a special and appreciated dynamics in everyday work.

By sharing important moments in establishing the corner stones of IBPT, and by being around whenever I needed their help, my dear colleagues from the Technical University of Denmark, Peter Weitzmann, Toke Rammer Nielsen and Ruut Peuhkuri, gave me invaluable support.

There are two persons to whom I would like to thank, Professor Johan Claesson at Chalmers University of Technology and Associate Professor Thomas Bednar at the Technical University of Vienna, for sharing with me their expertise in modeling and measuring of moisture transfer. I spent many valuable hours discussing with them. By insisting on some of key features in moisture transfer, they have directed my attention towards the most exciting problems in this area.

Professor Johan Claesson, together with my department colleagues Associate Professor Anker Nielsen and a fellow PhD colleague Björn Mattsson, contributed a lot with the critical reading of this manuscript.

The friendly and understanding environment I have enjoyed at the department, has helped me to experience a new culture and to become a jolly resident of the city of Gothenburg.

Finally, everything is possible with love and unconditional support from my family, my husband Srdjan and our daughter Katarina, who bravely follows her parents.

Contents

NOMENCLATURE .... **i**

Variables i
Subscripts iii
Constants iii

1. INTRODUCTION **1**

1.1 Scope of HAM-Tools **1**
1.1.1 HAM-Tools program structure. Main subsystems and the interface. 2
1.1.2 Program design in Simulink 4
1.1.3 HAM-Tools as a part of IBPT 6
1.1.4 Summary of the program capabilities 6

1.2 The relevance of HAM-Tools **7**
1.2.1 Building simulation tools at present 7
1.2.2 Trends in tools development 7
1.2.2.1 Code certification 8
1.2.2.2 Integrated simulation tools 9
1.2.2.1 CFD modeling 10

2. CALCULATION MODEL FOR THE HEAT, AIR AND MOISTURE TRANSPORT FOR THE WHOLE BUILDING **12**

2.1 One-dimensional heat, air and moisture transport in building enclosures **13**
2.1.1 Governing equations 13
2.1.2 Material properties 15

2.2 One-dimensional heat, air and moisture transport over a wall surface **19**
2.2.1 Exterior surface 19
2.2.2 Interior surface 20

2.3 Heat, air and moisture transport in internal air-zones **21**
2.3.1 Air balance model 21
2.3.2 Thermal model 22
2.3.3 Hygric model 24
2.3.4 Energy and moisture balance for the zone 24

3. NUMERICAL MODEL FOR THE BUILDING. HAM-Tools BLOCKS **25**

3.1 Building envelope **25**
3.1.1 External surface node 28
3.1.2 Internal (one) node 28
3.1.3 Internal surface node 29
3.1.4 Contact node 30
3.1.5 Air flow thorough the wall 31
3.1.6 Heat and moisture resistances in the wall 31

3.1.7 Material data 32

3.2 Internal air-zone 34

3.3 Environmental conditions 36

3.3.1 Weather file 36

3.3.2 Solar radiation model 36

3.3.3 Weather on surface 37

3.4 Sources 37

3.5 Whole building 37

4. SELECTED EXAMPLES OF THE APPLICATION OF THE CODE 41

4.1 Air transport in and around the building 41

4.1.1 Air transport through the wall 41

4.1.2 Air transport through the zone 42

4.2 Interstitial condensation – moisture transport over the contact surface 44

4.3 Rapid moisture transport through porous material 46

5. VALIDATION OF THE HAM-Tools 49

5.1 Analytical validation 49

5.2 Comparison with other codes 50

5.3 Empirical validation 53

6. CONCLUSIONS 60

7. FURTHER DEVELOPMENT 62

REFERENCES 64

NOMENCLATURE

Variables

Symbol	Unit	Description
A	m^2	Area
A_t	m^2	Total area ($A_t = \sum A_i$)
C	$J/K{\cdot}m^2$	Volumetric heat capacity of control volume
C_H	J/K	Volumetric heat capacity of room air
$C_{H,add}$	J/K	Additional volumetric heat capacity in room air, e.g. from furniture
C_M	kg/Pa	Volumetric moisture capacity of room air
c_p	J/kg·K	Specific heat capacity
$c_{p,s}$	J/kg·K	Specific heat capacity of dry material (solid matrix)
CF_{sol}	-	Convection factor of solar heat gains
D_w	m^2/s	Moisture diffusivity
d	m	Thickness of layer
Gnr	-	Number of attached gain blocks
g	kg/m^2s	Total moisture flow rate
g_{air}	kg/m^2s	Air flow rate
g_l	kg/m^2s	Liquid (water) flow rate
g_{rain}	kg/m^2s	Rain flow to surface
g_v	kg/m^2s	Water vapor flow rate
h_c	W/m^2K	Convective heat transfer coefficient
h_r	W/m^2K	Radiative heat transfer coefficient
I_{diff}	W/m^2	Radiation energy coming from diffuse solar radiation
I_{dir}	W/m^2	Radiation energy coming from direct solar radiation
I_{lw}	W/m^2	Long wave radiation energy
$M_{construction}$	kg/s	Moisture flow to the zone from construction elements
M_{gains}	kg/s	Moisture flow to the zone from gains
M_{vent}	kg/s	Moisture flow to the zone from ventilation systems
P_{air}	Pa	Air pressure
p_v	Pa	Partial pressure of water vapor in air
$p_{v,sat}$	Pa	Partial pressure of water vapor in air at saturation
Q_{air}	m^3/s	Air flow rate
$Q_{construction}$	W	Transmission heat losses

Symbol	Unit	Description
Q_{gains}	W	Heat gains to the room
Q_{solar}	W	Solar heat gains to the room
Q_{vent}	W	Ventilation heat losses
q	W/m^2	Density of heat flow rate
q_{air}	m^3/m^2s	Density of air flow rate
q_{cond}	W/m^2	Heat flow rate due to conduction
q_{conv}	W/m^2	Heat flow rate due to convection
q_{rad}	W/m^2	Net radiation energy absorbed by the opaque surface
q^g_{rad}	W/m^2	Net radiation energy absorbed by the glazing surface
R	$m^2{\cdot}K/W$	Heat flow resistance, or just resistance
R_{air}	$Pa{\cdot}s/m^3$	Air flow resistance
R_p	$m^2{\cdot}s{\cdot}Pa/kg$	Vapor flow resistance
R_s	m/s	Liquid moisture flow resistance
Snr	-	Number of attached construction blocks
Sysnr	-	Number of attached system blocks
s	Pa	Suction pressure
T	^oC	Temperature
t	s	Time
V	m^3	Volume
v	kg/m^3	Air humidity by volume
w	kg/m^3	Moisture content in a porous material
w_{cap}	kg/m^3	Capillary saturation moisture content
w_l	kg/m^3	Liquid moisture content
w_{sat}	kg/m^3	Vacuum saturation moisture content
x	m	Space coordinate
x_{air}	kg/kg	Moisture content in air
α_{sol}	-	Surface absorptivity of solar radiation
β_p	s/m	Convective water vapor transfer coefficient
δ_o	$kg/m{\cdot}s{\cdot}Pa$	Vapor diffusivity in air
δ_p	$kg/m{\cdot}s{\cdot}Pa$	Vapor permeability of porous material
δ_p^{exp}	$kg/m{\cdot}s{\cdot}Pa$	Vapor permeability of porous material, experimentally determined
ε	-	Surface emissivity
Φ_c	W	Convective part of heat sources in a room
Φ_r	W	Radiative part of heat sources in a room
ϕ	-	Relative humidity
λ	$W/m{\cdot}K$	Thermal conductivity
$\lambda_{m,l}$	s	Liquid moisture conductivity in porous material
λ_s	$W/m{\cdot}K$	Thermal conductivity of dry material
λ_T	$W/m{\cdot}K^2$	Thermal conductivity coefficient for temperature dependency

Symbol	Unit	Description
λ_w	$W \cdot m^2/kg \cdot K$	Thermal conductivity coefficient for moisture content dependency
μ'	-	Vapor resistance factor
ξ	kg/m^3	Specific moisture capacity
ρ_{air}	kg/m^3	Air density
ρ_o	kg/m^3	Density of dry material
τ	-	Transmittance of glazing surface
ψ_o	-	Open porosity

Subscripts

Symbol	Description
air	from surrounding air
air,ext	from outdoor (external) air
air,int	from indoor (internal) air
cond	conduction
conv	convection
ext	external
i,j,k	node or surface index
int	internal
left	left node or control volume
right	right node or control volume
ref	reference value
surf	surface

Constants

Symbol	Quantity	Unit	Description
$c_{p,air}$	1000	$J/kg \cdot K$	Specific heat capacity of dry air
$c_{p,l}$	4200	$J/kg \cdot K$	Specific heat capacity of water
h_e	$2.5 \cdot 10^6$	J/kg	Latent heat of evaporation
R_{H2O}	461.4	$J/kg \cdot K$	Gas constant of water vapor
ρ_l	1000	kg/m^3	Density of water
σ_s	$5.67 \cdot 10^{-8}$	$W/m^2 \cdot K^4$	Stefan-Boltzmann constant

1. INTRODUCTION

1.1 Scope of HAM-Tools

HAM-Tools is a building simulation software. ‘HAM’ stands for *H*eat, *A*ir and *M*oisture transport processes in a building and building envelope that can be simulated by this program, and ‘Tools’ describes its modular structure. The main objective of this tool is to obtain simulations of transfer processes related to building physics, i.e. heat and mass transport in buildings and building components in operating conditions. The tool is to be used as a research and educational tool for the investigation of the mechanism of above mentioned processes and of the degree of their correlation when they are coupled.

The general problem of the HAM-Tools simulations is depicted in Figure 1.1, where main systems and transfer processes involved are indicated. The scope of the simulation is to obtain transient HAM states of a building enclosure and indoor air, as a result of a building usage in specified operating conditions. This knowledge enables further analyses such as calculation of energy consumption of the building, indoor comfort assessment, risk analyses regarding moisture content levels in building construction and indoor air, functionality of HVAC systems, air flow distribution through openings on building enclosure, etc.

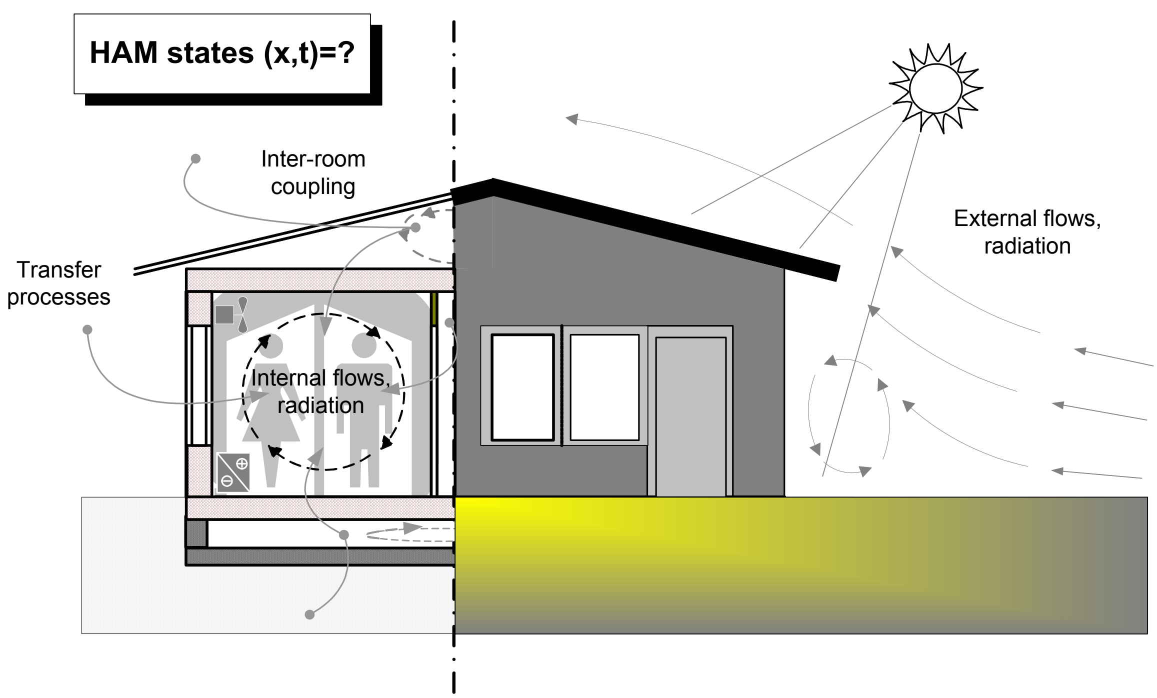

Figure 1.1 The HAM-Tools simulation problem.

1.1.1 HAM-Tools program structure. Main subsystems and the interface.

Based on the problem definition from Figure 1.1, five interacting systems may be identified: building construction, environment, indoor air, building services and occupants. These represent main subsystems in HAM-Tools simulations and they are named such as: ‘Construction’, ‘Weather’, ‘Zone’, ‘HVAC’ and ‘Gains’. Some possible relations between them are illustrated in Figure 1.2.

The ‘Construction’ system represents a building enclosure composed of walls, windows, etc. The ‘Weather’ system defines external climate load, i.e. outdoor operating conditions based on building position in space. The ‘Zone’ refers to an air volume of a room. The ‘HVAC’ system is a technical system which provides desired indoor climate through a certain input of heat, air and/or moisture. The ‘Gains’ system gives casual HAM inputs to the zone, which result from the building occupancy (from people living or working inside, appliances, etc). As it is indicated in Figure 1.2, physical properties of building materials should be known (‘Material database’). The same is valid for the weather data (‘Weather database’), which may be given in a form of a reference or a real (measured) climate for a specific location.

The systems interact in different ways. They ‘meet’ or ‘communicate’ with each other by exchanging data about present states. The way and degree of their coupling determine the data flow between them. For example, the HAM response of the Zone is governed by the magnitude of gains coming from the Construction, HVAC and Gains systems. Changes in HAM states of the Zone is registered by the HVAC system, which adjusts its next input, end so on.

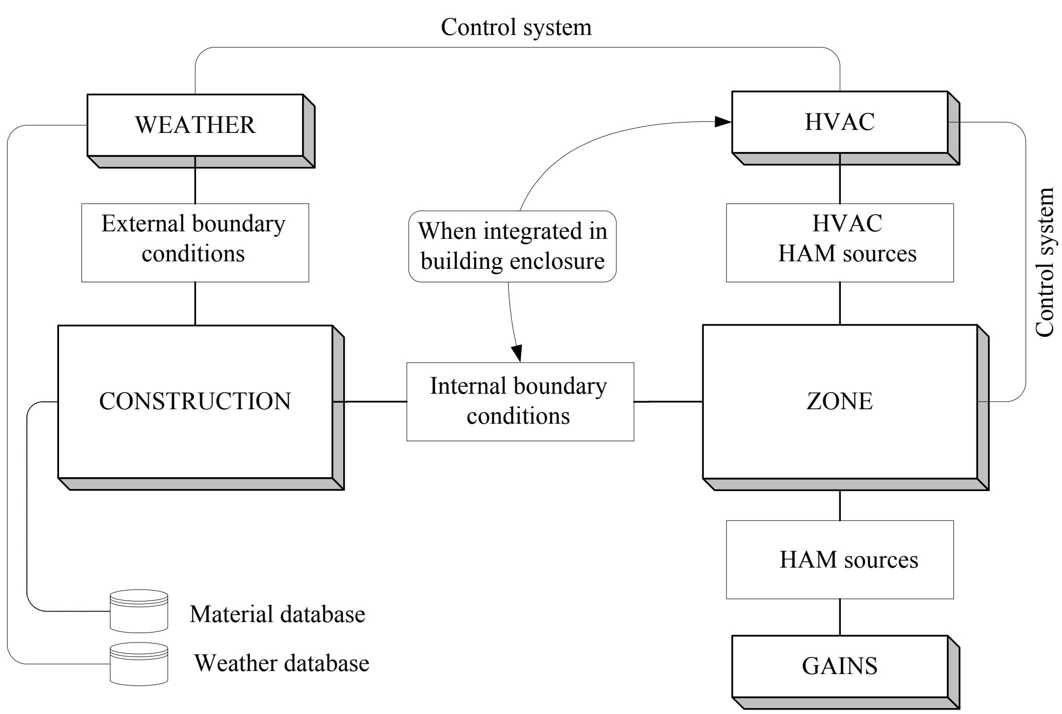

Figure 1.2 Main systems of the HAM-Tools simulation and the coupling scheme.

Communication ports between systems are denoted as: ‘External’ and ‘Internal boundary conditions’, ‘HVAC HAM sources’ and ‘HAM sources’, Figure 1.2. In order to enable the coupling of the systems, rules for data exchange over the meeting points must be defined. The set of such rules is called the interface. When all systems are coupled together and solved simultaneously, the resulting simulation represents a highest level of integration in HAM-Tools. For the highest level of integration, the rigid and definite interface is defined in form of seven data arrays (Rode et. al. 2002a):

Surface weather data array
Construction array
System array
Geometry array
Zone array
Radiation array
Gain array

By using the system of predefined arrays, the output from every subsystem is known, i.e. type and order of data in the array. Thus, the communication between systems is always ensured, even if they are developed separately from each other. As an illustration, the contents of the Construction array is given in Table 1.

Table 1 Construction array

Symbol	**Description**	**Unit**
R	Convective thermal surface resistance	m²· K/W
T_{surf}	Surface temperature	°C
R_p	Moisture surface resistance	m²·s·Pa/kg
$p_{v,surf}$	Surface vapour pressure	Pa
R_{air}	Air flow resistance	Pa·s/m^3
P_{air}	Air pressure of inlet airflow	Pa
Q_{solar}	Transmitted solar energy	W/m²
ε	Surface emissivity	-
T_{air}	Temperature of inlet airflow	°C
ϕ_{air}	Relative humidity of inlet airflow	-
Snr	Surface number	-

The general data flow chart organized by the signals from the above list is shown in Figure 1.3. Other couplings are also possible, such as when HVAC systems are controlled by parameters coming from the ‘Weather’ system (indicated in the Figure as dotted line). At the moment, the present signal structure fulfills modeling requirements in HAM-Tools. However, another signal arrangement may be required by future applications.

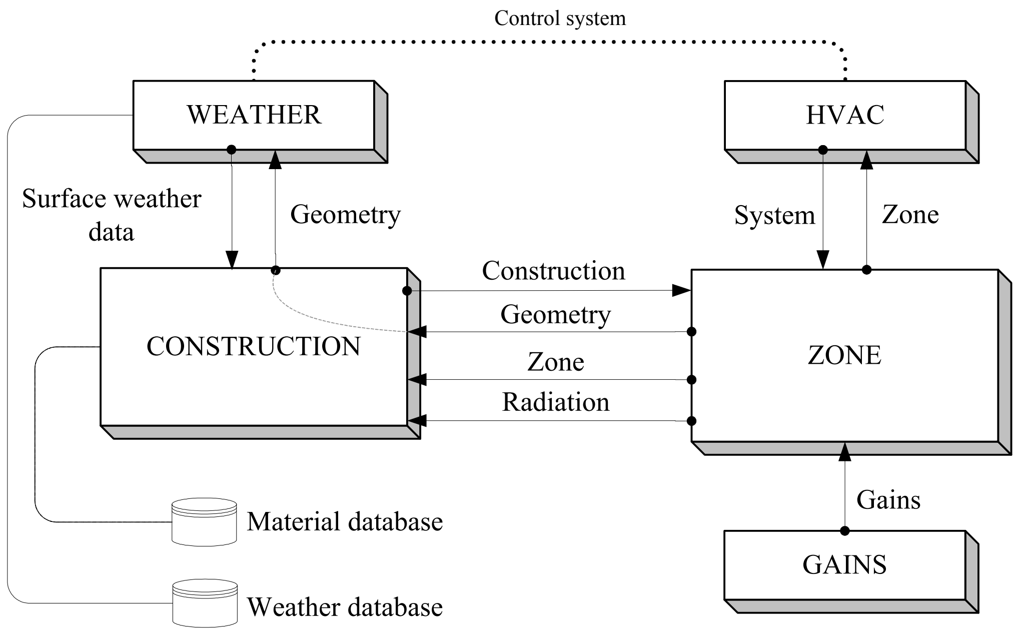

Figure 1.3 The system of seven communication arrays

1.1.2 Program design in Simulink

HAM-Tools program is constructed using a software package Simulink (MathWorks). Simulink is a graphical programming language, built on top of mathematical software package Matlab (MathWorks), for modeling, simulating and analyzing dynamic systems. The reason for choosing Simulink as a development environment was a large degree of flexibility, modular structure, transparency of the models and ease of use in the modelling process. Models in Simulink are built/drawn as block diagrams, in the same way as it would be done on paper. Modeling in Simulink is a process of assembling more complex blocks from the standard ones. A library of predefined blocks, which covers a variety of arithmetical functions, sinks, sources, linear and non-linear components and connectors, is provided in the package. As a part of the Matlab package, Simulink has built-in state-of-the-art ordinary differential equation (ODE) solvers, which are automatically configured at run-time of the model. Therefore, only a physical model needs to be implemented, and not the solver. This wide variety of modelling possibilities ensures that an optimal choice can always be made with respect to the task.

HAM-Tools is also a library of predefined elements, designed to serve as building physics calculation tools. Each block/tool from the library represents a certain part of the subsystem from Figure 1.2 or the subsystem as a whole. Therefore, tools are grouped according to their functionality into five categories:

Constructions	(external / internal walls and windows)
Zones	(air volume of the room, air cavity in a wall)
Systems	(HVAC systems)
Helpers	(handling of weather data and other basic blocks)
Gains	(internal heat and moisture gains)

In the Simulink graphical approach, the HAM-Tools library appears as it is shown in Figure 1.4, where the five subsystems appear as separate folders. Representatives of blocks from each of the subsystem are shown in the same figure below. Input and output connection ports that appear on the blocks are named according the signals they accept.

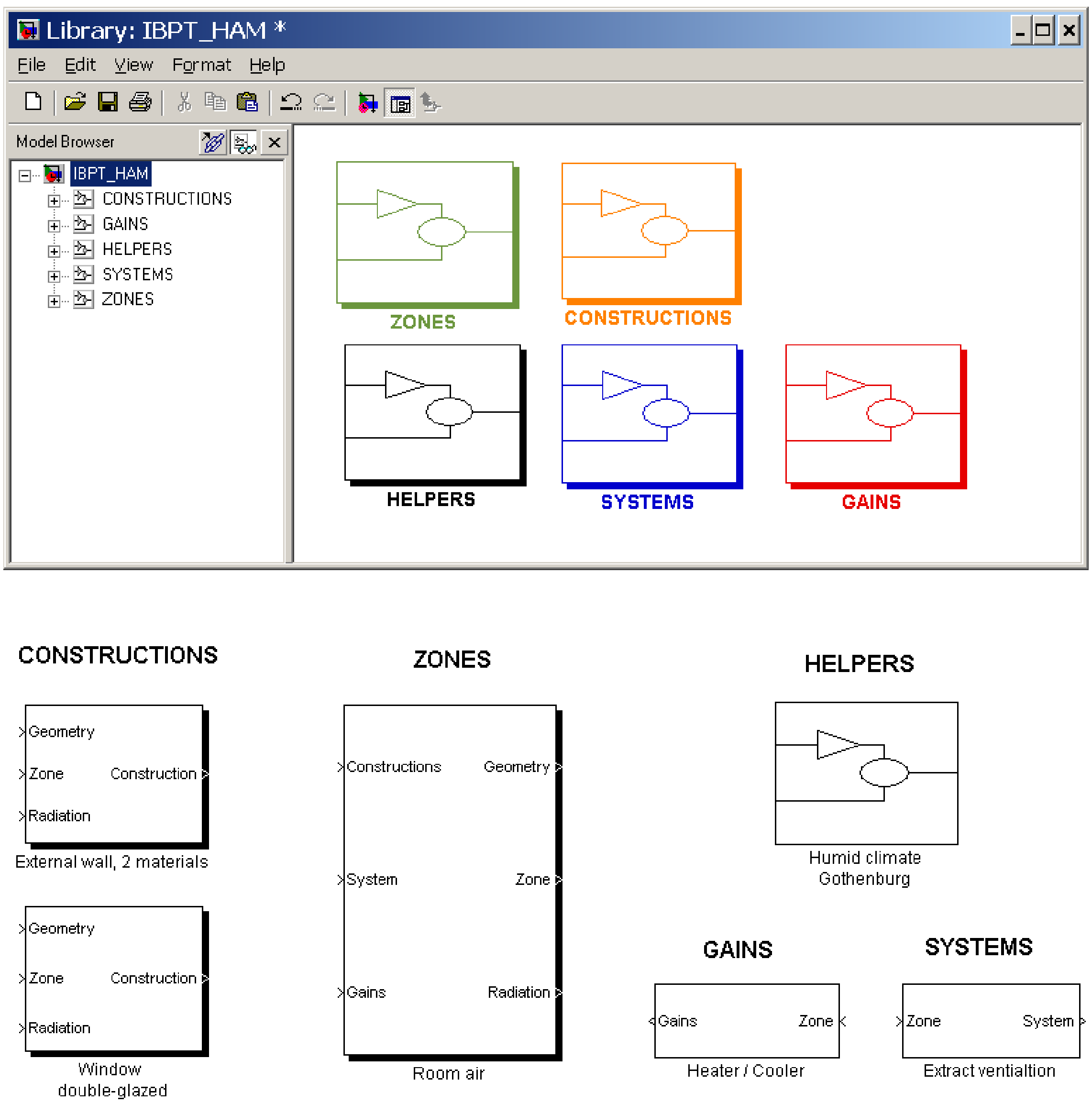

Figure 1.4 HAM-Tools library in Simulink, and some tools.

All models, including the ones presented, are hierarchical and open on every level. This means that each of the block diagrams may hide many other subsystems. This modular structure in Simulink - using systems and subsystems and the graphical approach, facilitate handling and control of a very complex interaction between different parts of the model. Other details about HAM-Tools block and their coupling are provided in sections that follow.

1.1.3 HAM-Tools as a part of IBPT

The HAM-Tools interface and the program structure are created together with the group of researchers from the Technical University of Denmark. Together with the program documentation, these are the corner-stones for the joint work around the International Building Physics Toolbox in Simulink (IBPT, 2002). These main designing rules are summarized in the IBPT 'General report' document, (Rode et.al. 2002 a). Examples of the successful and independent development of the IBPT library blocks are given in **Paper I** and **III**.

As the part of IBPT, HAM-Tools is an open research tool and publicly available for the free downloading. Any researcher can use, expand, and develop the contents of the toolbox.

1.1.4 Summary of the program capabilities

- 1D transient heat, air and moisture (HAM) transfer through the building enclosure.
- Transient HAM balance of the enclosed air, assuming well mixed air.
- Multi-zonal HAM calculations.
- Detailed modeling of internal HAM gains, originating from transmitted solar radiation, people, appliances, wind and temperature induced air flows through intentional and unintentional openings, with variable intensities and control strategies.
- Detailed modeling of the HVAC equipment (flows, pressure drops, control systems).
- Detailed modeling of the radiation heat exchange with surroundings based on the building orientation.
- Simplified modeling of the wind-induced air pressure distributions around the building and driving rain.

- Simplified modeling of the long-wave radiation exchange between internal surfaces.

- Possibility to couple to other codes / procedures for 2D and 3D HAM calculations.

1.2 The relevance of HAM-Tools

1.2.1 Building simulation tools at present

Computer simulations are widely used in a nowadays engineering practice and the building industry is, of course, a part of it. Building simulation tools contribute directly in building design and analysis. They help to assess the benefits of particular design, to improve life cycle performance, to enhance design quality, to link materials and health, to enable inter-disciplinary approach in design, and so on.

There are already about 300 registered energy-related building simulation tools (BES Tools Directory). They cover whole building analysis, materials, components, HVAC systems, codes and standards, lighting, air contaminants, etc. The real number is probably much higher. For example, among the ten Swedish codes registered at the cited place, six more are used in practice (see Bergsten, 2001).

Some codes are developed as simple engineering tools, providing fast and approximate solutions in an early design stage, while the others, known also as research tools, are more or sometimes extremely complex and require high user expertise in certain area(s). Besides engineering and research practice, university education is an important area where simulation tools are also widely used and developed.

From the research point of view, advanced computational tools have become almost an inseparable part of a nowadays research practice. Rapid development in computational technology initiates and supports faster development in scientific research and knowledge. Specialized computational tools allow, among other things, that more and more experiments can be done also on computers and not only in the field. Along with researchers, practitioners are also aware of the practical outcome of such experiments: simulations can provide qualitative information and in most cases they are much cheaper than field tests.

1.2.2 Trends in tools development

There are other, more concise analyses regarding the trends in tools development (see for example Augenbroe, 2001). As the author of this work, I take the freedom to select the following three: code certification, integrated simulation tools and CFD modeling. The selection is based on my personal observations.

1.2.2.1 Code certification

What can be done with a certain code and sometimes not with the others already available, is a natural question among practitioners. Since there are so many codes at the moment, there is a necessity for code certification, and the codes, just like any other product, can be labeled in a certain way.

This work has started in the seventies, by the establishment of the International Energy Agency (IEA). The IEA supports research and development in a number of areas related to energy. In one of these areas, Energy Conservation in Buildings and Community Systems (ECBCS), the IEA is sponsoring various exercises with the aim to predict more accurately the energy use of buildings, including comparison of existing computer programs and calculation methods. Up to now, 44 research projects, 'Annexes', have been initiated (ECBCS official internet site), and some of them, which are related to heat, air and moisture (HAM) calculation methodology for the building, are briefly presented here.

Annex 24, 'Heat-Air-Moisture Transport in highly Insulated new and retrofitted Envelope Parts' (HAMTIE), 1991-1995, offered the first concise overview of the existing models and codes for HAM transfer processes and effects in building enclosures. The first testing of the computational models was done through the inter-model comparison (Hens, 1996).

As a natural continuation of the Annex 24, the European Commission initiated '**HAMSTAD**' project (Heat, Air and Moisture Standards Development), 2000-2002, which focused on standardization procedures and the certification in this field. Instead of defining a system of deterministic and prescriptive pre-standards on modeling requirements for the development and commercialization of numerical codes, an 'open methodology' is proposed towards the European Standard CEN/TC89 WI 29.3. Among the other results, there are five benchmark cases that cover a whole range of HAM-related building design problems, (Hagentoft 2002a, 2002b).

Finally, the **Annex 41**, 'Whole Building Heat, Air and Moisture Response (MOIST-EN)' has started at the end of 2003. This Annex aims to provide a better understanding of the heat, air and moisture balance for the whole building.

At the moment, there is only one official certification test for the whole-building energy simulation programs – the BESTEST (Building Energy Simulation Test, Judkoff and Neymark, 1995). This test resulted from the IEA Annex 21, 'Environmental Performance of Buildings', 1988-1993. The BESTEST provides methodology for a systematical testing of simulation programs and diagnosing of the sources of predictive disagreement. The method consists of a series of test case buildings that progress systematically from simple to relatively realistic. Several reference programs were selected for the testing, representing the best state-of-the-art simulation capability among participating countries (Europe and USA). Results generated with the reference programs are intended to be useful for the evaluation of other building energy simulation tools.

The experience collected during the BESTEST development is worth presenting. It was shown that when a program exhibited a major disagreement with the reference programs, the cause was usually a bug, faulty algorithm or documentation problem, (Judkoff and Neymark, 1995). Bugs were found in all reference programs and it might be that they have been there for years. The fact that they were found during testing, shows the power and importance of the code validation. A large disagreement that remained even after all diagnosed problems were repaired, does not downgrade the test, but illustrates different assumptions in models and the need for further development.

The BESTEST is included in ANSI / ASHRAE Standard 140-2001.

1.2.2.2 Integrated simulation tools

The goal of the building design is to achieve high performance and multiple benefits at a low cost. This means that interests and requirements of all partners in the design process (investors, architects, construction, mechanical, electrical and environmental engineers, etc.), should be regarded simultaneously. Some examples of combined building envelope design and lighting strategies that significantly reduce the need for HVAC system requirements are given in Nilsson (2003). Since this approach integrates all partners during the whole phase, it is also called an integrated building design.

Integrated building simulation tools, such as integrated building design, provide a multi-disciplinary approach in assessing the design. This is accomplished by running several simulations in parallel, where each simulation represents an independent subsystem or an object. The core of the integrated software is the interface – the communication algorithm between components. Once well established, the interface allows running an arbitrary number of simulations, with arbitrary time-sequences. Furthermore, simulations (codes) can be developed separately from each other, with different levels of complexity. The code development requires specialists in the subject, but in most cases the application can be done by novice users.

Main systems (shadowed squares) and subsystems in building simulations are shown in Figure 1.5. Even if it looks challenging to compose the 'universal' tool that encloses all these systems, it is not necessary, and probably not possible if calculations are to be performed in reasonable time and with reasonable resources. Instead, the selection is usually made following the main interest, and other subsystems are either disregarded or represented in simplified but satisfactory ways. For example, such code can focus on energy consumption and human comfort aspects of the ventilation system, providing detailed calculations of airflow rates and airflow patterns in the system and internal zones; in addition, the distribution of air-contaminants can be also considered.

Some representatives of the integrated building simulation codes are ESP-r, IDA, Bsim2002 and EnergyPlus (BSE Tools Directory). Among these, modular tools such as SPARK, TRNSYS and IBPT are special for providing possibility to design new, non-standard elements, other then those included in the program, e.g. building integrated heating and cooling systems, ventilated facades, solar walls, etc.

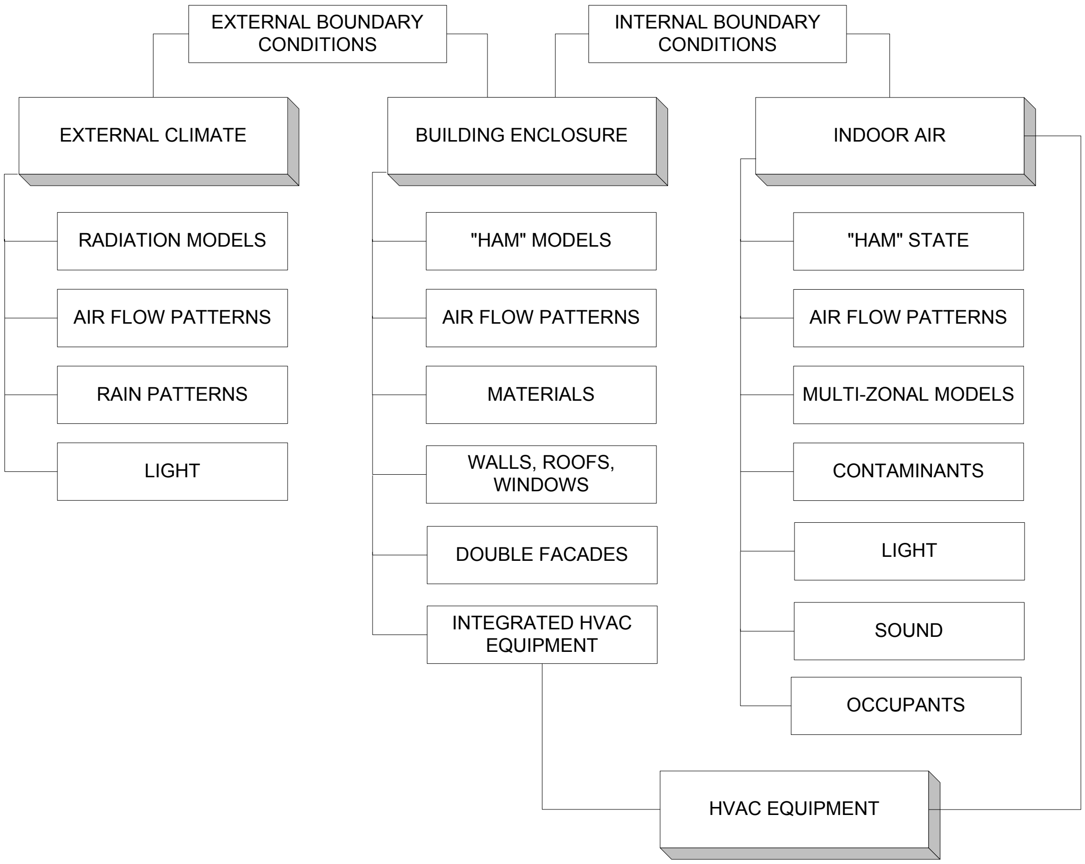

Figure 1.5 Main systems and subsystems of building simulation tools.

1.2.2.1 CFD modeling

Computational Fluid Dynamics (CFD) is a widely used term for the numerical solution, by computational methods, of the governing equations which describe the fluid flow: conservation equations for mass, momentum (described by Navier-Stokes equations) and energy. CFD programs are used to model fluid phenomena that cannot be easily simulated or measured with an experiment. Driving rain pattern on the building façade, (Blocken et.al. 2003a), wind flow patterns around the building (Blocken et.al. 2003b, Klemm et. al. 2003) or air convection through cracks and gaps in building envelope, Figure 1.6, are some of the newer examples from the building physics area. The application of CFD codes in engineering problems is very attractive, because of its possibilities, but complex. This kind of modeling requires expertise in physics, numerical methods and computation, to successfully apply CFD packages or to develop additional subroutines for specific problems. CFD simulations demand high computational capacity and sometimes are extremely time consuming. Compared to building simulation tools, a computational time scale used in CFD simulations is of another order – seconds, instead months or years. Some possibilities for applying CFD simulations in practice are seen through the integration with building simulation tools (Maliska, 2001).

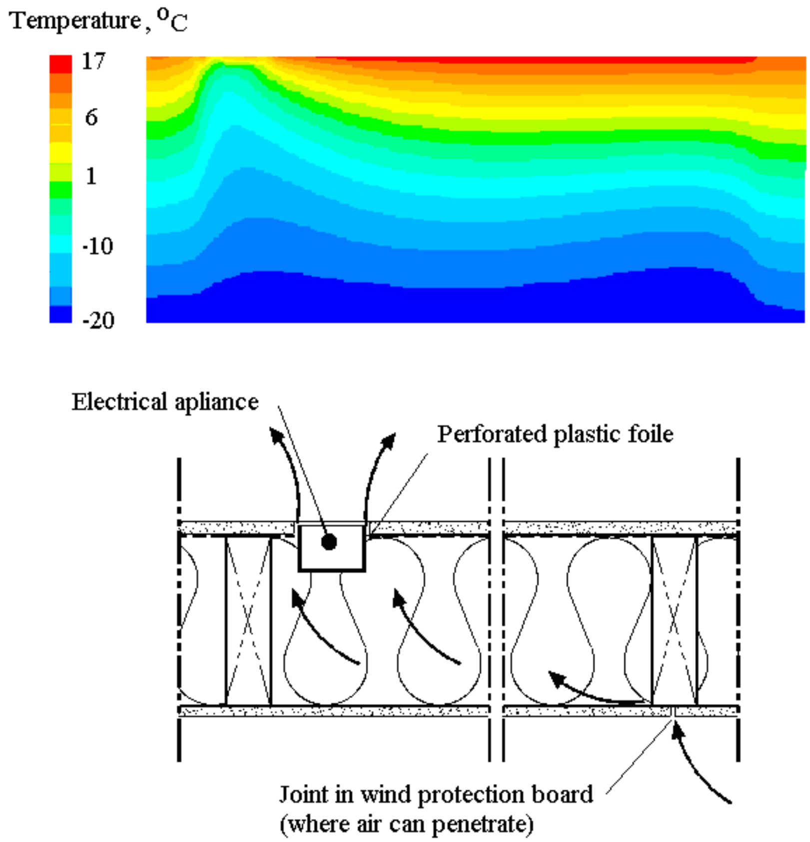

Figure 1.6 The figure shows 2D temperature field in an outer wall in winter time. An electrical appliance is inserted on internal side of the wall in a common way, with appropriate casement. As a result, an air barrier in the wall construction is ruined and the air leakage occurs around the casement forming the 'thermal bridge'. This spot is indicated with bended isotherms, unlike in undisturbed region where they are parallel. The simulation is made by my department colleague Björn Mattsson, using the CFD package 'Fluent'. Input data for the simulation are collected from measurements.

2. CALCULATION MODEL FOR THE HEAT, AIR AND MOISTURE TRANSPORT FOR THE WHOLE BUILDING

The calculation model for the whole building enclose governing equations for one-dimensional heat, air and moisture transfer in

- Building enclosures, i.e. HAM transport in porous building materials,
- Exterior and interior surfaces, and
- Internal air zones.

This model is incorporated in HAM-Tools 'Construction' and 'Zone' blocks. Besides the governing equations, the following thermal and moisture state relations are generally used:

The General gas law, which relates the partial pressure and humidity by volume:

$$\frac{p_v}{v} = R_{H2O} \cdot \left(T + 273.15\right) \tag{1}$$

The relative humidity is defined as:

$$\phi = \frac{p_v}{p_{v,sat}} \tag{2}$$

The calculation of the suction pressure, s, is approximated with the Kelvin's relation:

$$s = -\rho_l \cdot R_{H2O} \cdot (T + 273.15) \cdot \ln\phi \tag{3}$$

The water vapor saturation pressure is calculated as (according to Hens, 1996):

$$p_{v,sat} = exp\left(23.5771 - \frac{4042.9}{T + 273.15 - 37.58}\right), \quad 0 \le T \le 80^o C \tag{4}$$

and for $-30 \le T \le 0^o C$

$$p_{v,sat} = 611 \cdot exp\left(82.9 \cdot 10^{-3} \cdot T \quad - 288.1 \cdot 10^{-6} \cdot T^2 + 4.403 \cdot 10^{-6} \cdot T^3\right)$$

The vapor permeability of stagnant air (known also as Schirmer's equation):

$$\delta_o = \frac{26.1 \cdot 10^{-6}}{R_{H2O} \cdot (T + 273.15)} \tag{5}$$

2.1 One-dimensional heat, air and moisture transport in building enclosures

Governing equations for one-dimensional heat, air and moisture transfer and heat and mass balance in porous building materials are incorporated into the ‘Construction’ blocks. The presented model refers to the one described in Hagentoft (2002a). The model has the following limitations:

- Temperature should be in the range of –30 °C to +80 °C.
- Effects associated with phase change liquid from/to ice, are neglected.
- Climatic load due to driving rain is simplified.
- Hysteresis is not considered.
- Gravity effects are not considered.
- Chemical reactions are not considered.
- Drainage between material layers is not considered.
- Ageing effects or changes in geometrical dimensions are neglected.

2.1.1 Governing equations

Air flow through the structure is driven by the air pressure differences across the structure. The mass airflow rate, g_{air}, is assumed constant through the whole structure, allowing for variations in time.

$$g_{air} = \rho_{air} \cdot q_{air} \tag{6}$$

The volumetric airflow rate, q_{air}, is a function of the air pressure difference, ΔP_{air}. The air flow is positive when it is directed towards interior.

Heat flow is divided into a conductive and a convective part:

$$q = q_{cond} + q_{conv} \tag{7}$$

The conductive part is proportional to the gradient of the temperature:

$$q_{cond} = -\lambda \frac{\partial T}{\partial x} \tag{8}$$

where the thermal conductivity, λ, is the coefficient of proportionality. The convective part is modeled as the sum of sensitive specific enthalpy flow of the air and latent specific enthalpy flow of the vapor:

$$q_{conv} = g_{air} \cdot c_{p,air} \cdot T + g_v \cdot h_e \tag{9}$$

The reference temperature is zero, and thus the sensible specific enthalpy at 0 ^{o}C is zero. The first part is present only if the air flow is taken into account. The enthalpy flows that originate from vapor and liquid flows are neglected.

Moisture flow. For the sake of modeling, it is assumed that the total moisture flow can be divided into two parts, one resulting from the vapor diffusion, and the other originating from the liquid moisture transport:

$$g = g_v + g_l \tag{10}$$

The water vapour partial pressure, p_v, is used as the state variable for the vapor transport and suction pressure, *s,* for the liquid transport.

The liquid flow is proportional to the gradient of the suction pressure:

$$g_l = \lambda_{m,l} \cdot \frac{\partial s}{\partial x} \tag{11}$$

where $\lambda_{m,l}$ is the hydraulic conductivity. Due to the definition of the suction pressure (Equation 3), the minus sign is omitted in this formulation.

The vapor flow consists of a diffusive and a convective part:

$$g_v = -\delta_p \cdot \frac{\partial p_v}{\partial x} + g_{air} \cdot x_{air} \tag{12}$$

The diffusive part is proportional to the gradient of the water vapor partial pressure (Fickian diffusion) with the vapor permeability δ_p, as the coefficient of the proportionality. The convective part exists only if the air flow is taken into account, in which case the water vapor content, x_{air}, is approximated by the following equation:

$$x_{air} = \frac{0.621 \cdot p_v}{P_{air} - 0.379 \cdot p_v} \approx 6.21 \cdot 10^{-6} \cdot p_v \tag{13}$$

All flow coefficients, λ, δ_p and $\lambda_{m,l}$, for the heat and for the moisture transfer are normally dependent on the temperature and moisture conditions of the material.

Energy and moisture balances are given with following relations:

$$-\frac{\partial q}{\partial x} = c_p \cdot \rho_s \cdot \frac{\partial T}{\partial t} \tag{14}$$

$$-\frac{\partial g}{\partial x} = \frac{\partial w}{\partial t} \tag{15}$$

2.1.2 Material properties

Specific heat capacity for porous material is defined as:

$$c_p = c_{p,s} + \frac{1}{\rho_s} \cdot c_{p,l} \cdot w_l \tag{16}$$

where c_s, refers to dry material and c_l, refers to water within the pores. The heat capacity of the existing water vapor in the pores is neglected.

Thermal conductivity reads:

$$\lambda = \lambda_{s,ref} + \lambda_T \cdot \left(T - T_{ref}\right) + \lambda_w \cdot \left(w - w_{ref}\right) \tag{17}$$

where $\lambda_{s,ref}$ refers to dry material at the reference temperature T_{ref}, and λ_T and λ_w are correcting coefficients for the deviations in temperature and moisture states from the reference ones.

Retention curves give relation between the moisture content of a material and the relative humidity of a surrounding air. These curves can be defined with the following relations:

$$w(\phi) \text{ or } \phi(w) \tag{18}$$

in which case they are called sorption curves, or as water retention curves:

$$w(s) \text{ or } s(w) \tag{19}$$

Necessary transformations between sorption and water retention curves can be performed using the relation given by Equation 3.

Moisture uptake and release is characterized by hysteresis and because of that there are two boundary retention curves, as it is shown in Figure 2.1. Wetting of a dry material follows the lower curve, which is called ‘wetting’ or ‘absorption’ curve. Drying of a wet material follows the upper one, denoted as ‘drying’ or ‘desorption’ curve. Since the hysteresis is neglected in the present model, the moisture retention is described with one of the curves, or as the most appropriate, with the curve defined as being between them. Some characteristic states for the moisture retention, which will be refereed to later in the text, are denoted on the diagram on the right. A maximum moisture content that can be achieved during wetting is denoted as w_{cap}. Even higher moisture content, w_{sat}, can be achieved if material is exposed to the wetting long enough, so the air entrapped in pores can dissolute in the water. There is a certain relative humidity (usually close to 95 %) when the liquid moisture transport becomes a dominant mechanism in the total moisture transport. The corresponding moisture content is denoted with w_{lim}. The dry moisture content, w_{dry} is actually the zero moisture content or close to zero. Other characteristic regions are defined in Figure.

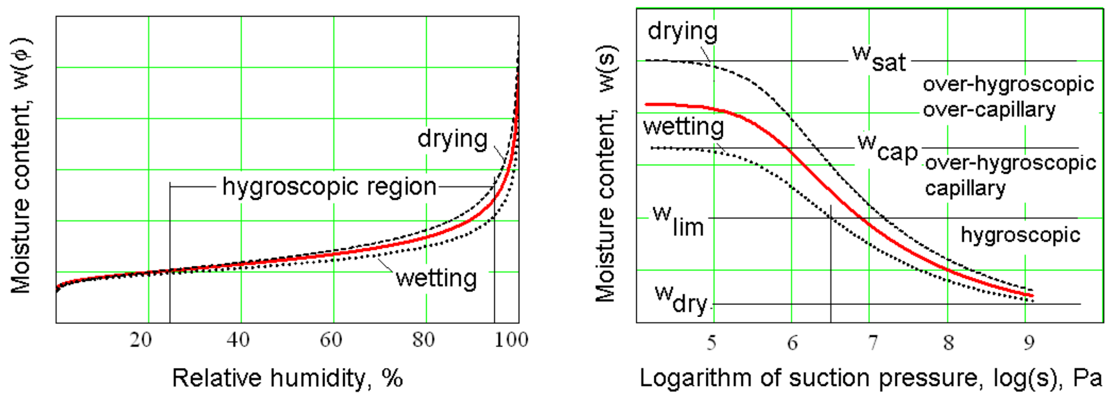

Figure 2.1: Sorption curve (left) and water retention curve (right). Regimes of moisture storage in hygroscopic capillary-active materials, according Carmelite and Roels (2002).

Specific moisture capacity, ξ, is defined as the increase in the mass of moisture in unit mass of the material, that follows the unit increase in the relative humidity:

$$\xi(\phi) = \frac{\partial w}{\partial \phi} \tag{20}$$

Moisture transfer coefficients, i.e. water vapor permeability (δ_p, Equation 12) and liquid water conductivity ($\lambda_{m,l}$, Equation 11), should describe vapor and liquid water flux separately. This model is based on the assumption that vapor flux through porous material is linearly proportional to volume of pores filled with (humid) air. Vapor diffusion is a dominant mechanism of moisture transfer in the region with lower relative humidities, Figure 2.1. As the moisture content of the material increases towards the capillary saturation, the pores filled with condensed water outnumber the ones filled with air. In turn, the liquid transfer becomes the dominant mechanism, while the vapor transfer decreases to zero. The functional forms of the vapor diffusivity and the liquid conductivity are illustrated in Figure 2.2.

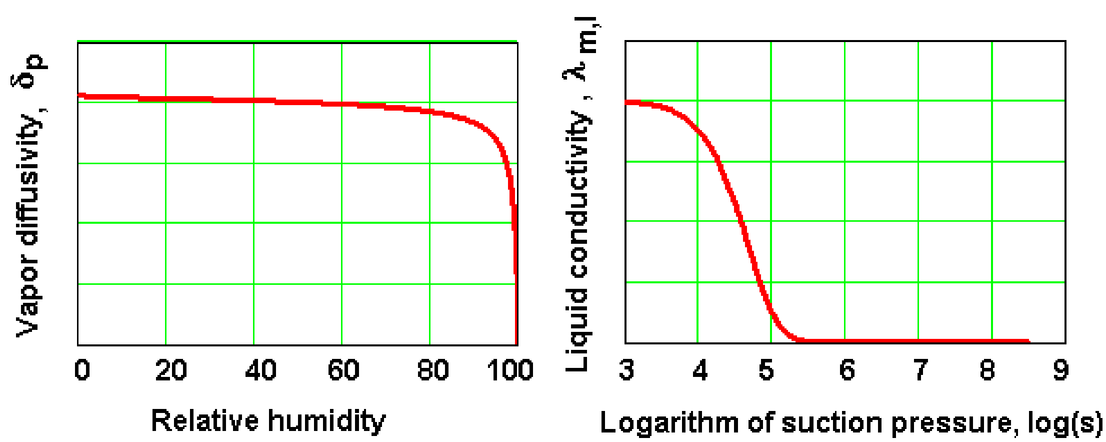

Figure 2.2 The functional forms of vapor diffusivity and liquid conductivity.

There are two difficulties in preparing the moisture transfer properties to the form required by this model. The first one is that these transport properties are not directly measurable by standard experimental methods, and thus have to be estimated from other measured properties. The second difficulty is that measurements are usually performed under isothermal conditions which means that obtained transfer properties correspond to that reference temperature. When applied to the non-isothermal cases, these properties may introduce additional uncertainties in simulations. Further explanations regarding both problems are provided hereafter.

Measured moisture transport properties

There are several experimental techniques for measuring moisture transport properties. They can roughly be divided into: gravimetrical methods, such as the well known 'cup' tests; scanning techniques, like nuclear magnetic resonance, gamma-ray or x-ray attenuation; and others (see for example Jantz, 2000). By applying any of these methods, only a total moisture flow can be measured, and therefore, only a total transport property can be evaluated.

For example, experimentally determined water vapor diffusivity by 'cup' tests, δ_p^{exp}, is calculated from the following equation:

$$g \cdot d = \delta_p^{\exp} \cdot A \cdot \Delta p_v \tag{21}$$

where d and A are the thickness and area of the specimen respectively, g is the moisture flow rate through the area A, and Δp is a difference in water vapor pressure across the specimen surfaces. The moisture flow rate is gravimetrically determined under isothermal, steady-state conditions, with known values of boundary relative humidities. The method is applicable in the hygroscopic region (Figure 2.1). Since both vapor and liquid flow may be active within this range of relative humidities, the measured flow represents the total moisture flux. Cup tests are standardized experimental methods, (EN ISO 12572), and vapor permeability obtained in this way is usually available in material databases.

Moisture diffusivity is another transport property in material databases, which describes moisture transfer at higher moisture levels. It is determined from sets of experiments where one side of the specimen is in direct contact with the water. Due to the existence of the water concentration gradient, water diffuses into the specimen. The distribution of moisture within the specimen is determined as a function of time at various intervals. Choosing the moisture content as the state variable, the moisture diffusivity, D_w, can be estimated from the total measured moisture flow:

$$g = -D_w \cdot \frac{\Delta w}{\Delta x} \tag{22}$$

This diffusivity is sometimes denoted as the 'liquid moisture diffusivity'.

While the 'liquid diffusivity' may truly represent the liquid transfer coefficient in the over-hygroscopic region (assuming that the vapor transfer is negligibly low compared to the liquid one), it is definitely incorrect to assume the same for measured 'water vapor permeability'. The experimentally determined water vapor diffusivity from Equation 21 increases with increse of the mean relative humidity of the specimen, affected by the liquid transport. It should be just opposite for the model presented. Comparing Equation 21 with Equation 12 (and assuming no air convection), the difference between experimentally determined water vapor permeability and the one defined in this model is evident.

In the work of Galbraith et. al. (2003), an alternative measuring method for the moisture transfer coefficients is presented. This new approach involves gravimetric tests within an environment of reduced barometric pressure. By assuming that the vapor diffusion coefficient is inversely proportional to the total air pressure, and that liquid permeability is not, it is possible to obtain separated flow coefficients, i.e. vapor and liquid permeability, as they are defined in this thesis. Their measurements on three selected materials (lightweight aggregate concrete, cement mortar and medium density fiberboard) have shown that the vapor transfer coefficient decreases at higher relative humidities, and the one for the liquid increases, which is also in accordance with the model presented.

However, the most of publicly available material databases still provide data for the total moisture transfer coefficients, (Kumaran 1996, ASHRAE 2002), and for the sake of a future user of HAM-Tools, it necessary to explain the flow separation procedure.

<u>The flow separation procedure</u>

The flow separation procedure can be done in the following way. Basically, it is assumed that the vapor flow through a porous medium can be compared to the vapor diffusion in stagnant air, δ_o (Equation 5):

$$\delta_p(w) = \delta_o \cdot \frac{1}{\mu'} \cdot f(w,...) \cdot \left(1 - \frac{w}{w_{sat}}\right) \tag{23}$$

with the vapor resistance factor μ', as the factor of proportionality. This factor describes the pore structure of the material, illustrating how many times lower the vapor diffusion in the porous medium is than in air. By the definition, μ' for stagnant air is equal to unity. If the layer of the porous material is assumed with pores connecting two parallel bounding surfaces of the material straight across, and if each pore is uniform with respect to the cross-sectional area (Kumaran, 1996), then μ' can be defined as:

$$\mu' = \frac{1}{\psi_o} \tag{24}$$

where ψ_o represents the open porosity, i.e. the volume of pores per unit volume of the material, accessible for water vapor. In practice, μ' value can be calculated from Equation 23, when the vapor permeability of the dry specimen is known.

The third term in Equation 23, gives other corrections to the μ' value, such as in the case with non-uniform and randomly directed pores (referred to as tortuosity).

The last term, $(1 - w/w_{sat})$ ensures that the vapor flow is stopped when the moisture saturation is reached (all pores are filled with water). The functional form of vapor permeability according to Equation 23 is presented in Figure 2.2. From this (assumed) form of the vapor permeability and from experimentally evaluated total transport coefficients (Equations 21 and 22), it is possible to calculate the liquid water conductivity using Equations 10-12.

Moisture flow coefficients for non-isothermal cases

Note that the total transport coefficients are usually evaluated under isothermal conditions. Consequently, the procedure presented for the flow separation will provide a unique solution to the moisture distribution inside the material only for the reference isothermal case, i.e. under the conditions from the measurements. By varying the form of Equation 23, different vapor diffusivity and liquid water conductivity can be achieved for the same material, resulting in different solutions for the moisture distribution under non-isothermal conditions.

Thus, the first assumption in this procedure, Equation 21, should be additionally tested from the measurements performed under non-isothermal, possibly steady-state conditions, such as the ones performed by Segerholm (2004). In the steady-state, the net moisture flux over a material specimen is constant:

$$g = g_v + g_l = const \qquad (25)$$

The calculated vapor and liquid flows (with the assumed moisture transfer coefficients) should fulfill this equation, and by that, the calculated temperature and moisture content distribution along the specimen should correspond to the values obtained by measurements. When such data are not provided, the vapor diffusivity from Equation 23 is applied to non-isothermal cases, and then the uncertainty, whether it is correct or not, remains. This problem is also pointed out by other researchers (for example Claesson 1993, Grunewald 2001, Jantz, 2002).

2.2 One-dimensional heat, air and moisture transport over a wall surface

This section includes one-dimensional heat, air and moisture transport equations for the exterior and interior wall surface. The presented models are incorporated in 'External surface' and 'Internal surface' blocks from the 'Helpers' library, which are parts of the 'Construction' block assembly.

2.2.1 Exterior surface

External wall surfaces are exposed to the convective heat and moisture exchange with outdoors air, incident solar radiation, long-wave radiation, transfer of latent heat, air and rain.

Heat flow to the surface, q_{ext}, from the surrounding, is given by the following equation:

$$q_{ext} = h_c \cdot \left(T_{air,ext} - T_{surf}\right) + q_{rad,ext} + \left(g_{air} \cdot c_{p,air} + g_{rain} \cdot c_{p,l}\right) \cdot T_{air,ext} + g_v \cdot h_e \quad (26)$$

The first two terms represent the convective and radiative heat exchange with the surrounding air. The third and the fourth parts refer to the specific enthalpy flows for the air and water, when either the air infiltration or the rain is taking place. The reference temperature is zero, and thus the sensible specific enthalpy at the reference temperature is zero. The specific enthalpy flow for the water vapor is presented only by the latent part, the last term, while the sensitive part is neglected.

If the air is flowing out from the structure (ex-filtration), the above equation reads:

$$q_{ext} = h_c \cdot (T_{air,ext} - T_{surf}) + q_{rad,ext} + g_{air} \cdot c_{p,air} \cdot T_{surf} + g_v \cdot h_e \quad (27)$$

It is assumed that no liquid water can leave the structure.

Net radiant energy absorbed by the wall surface originates from the incoming solar radiation (direct and diffuse parts) and long-wave radiation exchange with surroundings:

$$q_{rad,ext} = \alpha_{sol} \cdot \left(I_{dir} + I_{diff}\right) + \varepsilon \cdot \left(I_{lw} - \sigma_s \cdot T_{surf}^4\right) \quad (28)$$

The positive sign in the formulas is used when the flow is directed into the house.

Moisture flow to the surface can be in the form of the vapor or liquid flow. The vapor flux, g_v , reads:

$$g_v = \beta_p \cdot \left(p_{v,air,ext} - p_{v,surf}\right) + \begin{cases} g_{air} \cdot x_{air,ext}, & g_{air} > 0 \\ g_{air} \cdot x_{air,surf}, & g_{air} < 0 \end{cases} \quad (29)$$

where g_{air} gives the mass flow of the air, in the presence of the air filtration. The index $p_{v,air,ext}$ refers to the ambient water vapor pressure. The sign of g_{air} is positive when air is flowing into the house.

Suction of water from driving rain can take place for capillary active surface materials. The liquid inflow becomes the minimum of

$$g_l = \lambda_{m,l} \cdot \frac{\partial s}{\partial x}, \quad x = 0 \quad (30)$$

and the prescribed flow g_{rain}.

2.2.2 Interior surface

The heat flux to the internal surface, q_{int}, from the internal air is modeled as:

$$q_{int} = h_c \cdot (T_{air,int} - T_{surf}) + q_{rad,int} + g_{air} \cdot c_{p,air} \cdot T_{air,int} + g_v \cdot h_e \quad (31)$$

when the air is flowing into the construction from interior (ex-filtration). For the case of air flowing out from the wall, the heat flux reads:

$$q_{int} = h_c \cdot (T_{air,int} - T_{surf}) + q_{rad,int} + g_{air} \cdot c_{p,air} \cdot T_{surf} + g_v \cdot h_e \quad (32)$$

Net radiant energy absorbed by the wall surface is calculated according Equation 46, Section 2.3.

Moisture flow to the surface, i.e. the vapor flux, g_v , reads:

$$g_v = \beta_p \cdot \left(p_{v,air,int} - p_{v,surf}\right) + \begin{cases} g_{air} \cdot x_{air,surf}, & g_{air} > 0 \\ g_{air} \cdot x_{air,int}, & g_{air} < 0 \end{cases} \tag{33}$$

where $p_{v,air,int}$ refers to the ambient water vapor pressure. The sign of g_{air} must be also kept in mind (and is opposite to the case of the external wall surface).

2.3 Heat, air and moisture transport in internal air-zones

Temperature, relative humidity and pressure of the internal air are defined by the heat, air and moisture gains through the building enclosure, HVAC systems and other sources (other intentional or unintentional sources, not enclosed in HVAC systems). The presented system of the governing equations for the heat, air and moisture balance for the air-zone, is incorporated in the 'Zone' block, from the library with the same name. The model assumes well mixed air (one air node). Long wave radiation exchange between surfaces is taken into account in a simplified way.

2.3.1 Air balance model

The airflow through a zone is governed by pressure differences that exist across construction elements or is caused by an air handling unit:

$$\Delta P_{air} = P_{air,ext} - P_{air,int} \tag{34}$$

All airflows through the zone are defined by the pressure difference and the airflow resistance:

$$Q_{air} = \frac{\Delta P_{air}}{R_{air}} \tag{35}$$

The indoor air pressure is calculated from the balance equation for all flows in and from the zone:

$$\sum_k Q_{air,k} = 0 \tag{36}$$

Flows are defined as positive when they are directed into the zone.

2.3.2 Thermal model

Thermal model of a zone is based on the WAVO (de Witt, 2000). The model is developed with these assumptions:

- Room air has uniform temperature.
- Surface transfer coefficients for radiation are constant.
- View factors are approximated with integrating sphere values (long-wave radiation is equally distributed over the walls).
- All radiative heat inputs (short wave and emitted long wave) are distributed in such a way that all surfaces, except windows (glazing), absorb the same amount of that energy per unit of surface area.

Heat flow to the zone

Transmission heat losses:

$$Q_{construction} = \sum_{i=1}^{Snr} \frac{A_i \cdot \left(T_{air,int} - T_{surf,i}\right)}{R_i} \tag{37}$$

Ventilation heat losses:

$$Q_{vent} = \rho_a \cdot c_{p,air} \cdot \sum_{k=1}^{Sysnr+Snr} Q_{air,k}\Big|_{>0} \cdot \left(T_{air,ext,k} - T_{air,int}\right) \tag{38}$$

where $Q_{air,k}\Big|_{>0}$ are all positive airflows into the zone.

Heat sources in the zone

Depending on the heating (cooling) plant type, the heat supply is split into a convective and a radiative part. This is also done for casual and solar gains.

Solar heat gains coming through glazing areas:

$$Q_{solar} = \sum_{i=1}^{Snr} \tau_i \cdot \left(I_{dir} + I_{diff}\right)_i \cdot A_i \tag{39}$$

Heat gains coming from the heating system or casual gains (they are already divided in the convective and radiative part at the input to the zone[1]):

[1] For example, the convective part for an air heating system is 1 (or 100% of the total input), and 0.7 (70%) for a hydronic one.

$$Q_{gains} = \sum_{l=1}^{Gnr} \left(Q_{gains,conv} + Q_{gains,rad}\right)_l \tag{40}$$

The convective part of all heat sources is:

$$\Phi_c = CF_{sol} \cdot Q_{solar} + Q_{gains,conv} \tag{41}$$

where CF_{sol} represents the convective fraction of solar heat gains. The radiative part of all heat sources is:

$$\Phi_r = \left(1 - CF_{sol}\right) \cdot Q_{solar} + Q_{gains,rad} \tag{42}$$

<u>Radiation heat exchange at internal surfaces</u>

In addition to the radiation coming to the zone from different sources, there is a radiation emitted by each surface in the zone. The total surface radiation is equal to:

$$\sum_{j=1}^{Snr} A_j \cdot \varepsilon_j \sigma_s \cdot \left(T_{surf,j} + 273.15\right)^4 \tag{43}$$

It is assumed that this sum is equally spread over all inner surfaces. As each surface also emits radiation, the net radiation exchange is:

$$\frac{\sigma_s \cdot \sum_{j=1}^{Snr} A_j \cdot \varepsilon_j \cdot \left(T_{surf,j} + 273.15\right)^4}{A_t} - \sigma_s \cdot \varepsilon_i \left(T_{surf,i} + 273.15\right)^4 \tag{44}$$

In linearized form, this expression reads

$$h_r \cdot \left(T_{surf,mean} - T_i\right) \tag{45}$$

where h_r is the surface heat transfer coefficient due to radiation. This coefficient is assumed to be 6 W/m^{2}K for all surfaces.

The net radiation coming to each surface is calculated as:

$$q_{rad,i} = \frac{\Phi_r}{A_t} + h_r \cdot \left(T_{surf,mean} - T_i\right) \tag{46}$$

For glazing surfaces, a part of the incoming solar radiation is transmitted back through the glazing, so the net radiation energy for the glazing, $g^{g}_{rad,i}$, reads:

$$q^{g}_{rad,i} = q_{rad,i} - \left(1 - CF_{sol}\right) \cdot \frac{Q_{sol}}{A_t} \tag{47}$$

2.3.3 Hygric model

Moisture flows in the zone

Vapor diffusion from/to construction elements:

$$M_{construction} = \sum_{i=1}^{Snr} \frac{A_i \cdot \left(p_{v,air,int} - p_{v,surf,i}\right)}{R_{p,i}} \tag{48}$$

Vapor infiltration through ventilation systems:

$$M_{vent} = 6.21 \cdot 10^{-6} \cdot \rho_{air} \cdot \sum_{k=1}^{Sysnr+Snr} Q_{air,k}\Big|_{>0} \cdot \left(p_{v,air,ext,k} - p_{v,air,int}\right) \tag{49}$$

where $Q_{air,k}\Big|_{>0}$ are all positive airflows to the room.

Moisture gains (from people, appliances, etc.):

$$M_{gains} = \sum_{l=1}^{Gnr} constant\ or\ function\ defined\ by\ user, (kg \cdot s) \tag{50}$$

2.3.4 Energy and moisture balance for the zone

The energy balance equation reads:

$$C_H \cdot \frac{dT_{air,int}}{dt} = Q_{constructions} + Q_{vent} + \Phi_c \tag{51}$$

where C_H represents volumetric heat capacity of the air in the zone, which is calculated by the equation

$$C_H = \rho_{air} \cdot c_{p,\,air} \cdot V + C_{H,add} \tag{52}$$

and $C_{H,add}$ is additional heat capacity in the zone, due to for example furniture.

The moisture balance equation reads:

$$C_M \cdot \frac{dp_{v,air,int}}{dt} = M_{constructions} + M_{vent} + M_{gains} \tag{53}$$

where C_M is volumetric moisture capacity of the air in the zone given by the following equation:

$$C_M = 6.21 \cdot 10^{-6} \cdot \rho_{air} \cdot V \tag{54}$$

The moisture content in the air is limited to the saturation value $v_{air,sat}(T)$. In the case that this level is exceeded, it is assumed that the condensed amount of water is taken by some other sink, as well as a released heat.

3. NUMERICAL MODEL FOR THE BUILDING. HAM-Tools BLOCKS

A system of energy and mass balance equations from Section 2, for heat, air and moisture transfer in a building and a building envelope is solved numerically using the control volume technique and explicit time discretization scheme.

This section encloses discretized form of governing partial differential equations for a building envelope and an internal air zone, followed by calculation models for environmental conditions and sources of mass and energy to the building. Finally, a numerical model for the whole building is presented as a combination of these.

3.1 Building envelope

A building envelope is regarded as an arrangement of multi-layer walls and windows. Some basic construction assemblies, like an external wall, an internal 'sandwich' wall and a doubled glazed window are provided as pre-defined blocks in the 'Constructions' library. All these blocks are designed as a combination of other (basic) blocks, called:

Weather on surface
External surface node
One node
Internal surface node
Contact node
Air flow through construction
Resistances

Since these blocks 'help' in modeling of a construction element, they are placed in the 'Helpers' library.

A numerical model for each of the stated basic blocks, except 'Weather on surface', is presented in this section. As an illustration of the modeling process, a numerical model for an external two-material wall is given in Figure 3.1; the corresponding model in Simulink, using the 'Helpers' blocks, is given in Figure 3.2. The block 'Weather on surface' is presented in Section 3.3, 'Boundary conditions'.

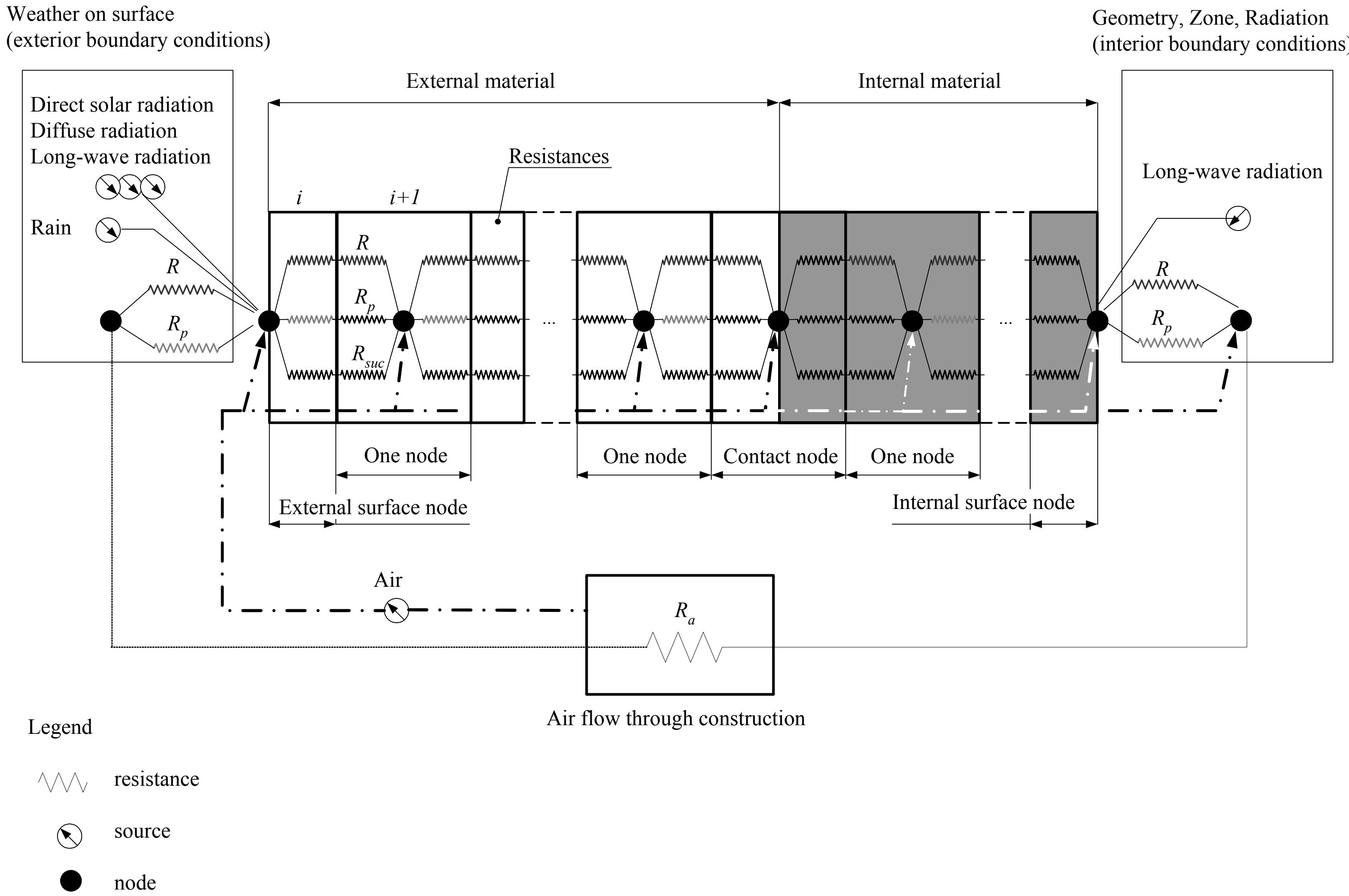

Figure 3.1 Numerical model of an external wall, made of two different materials.

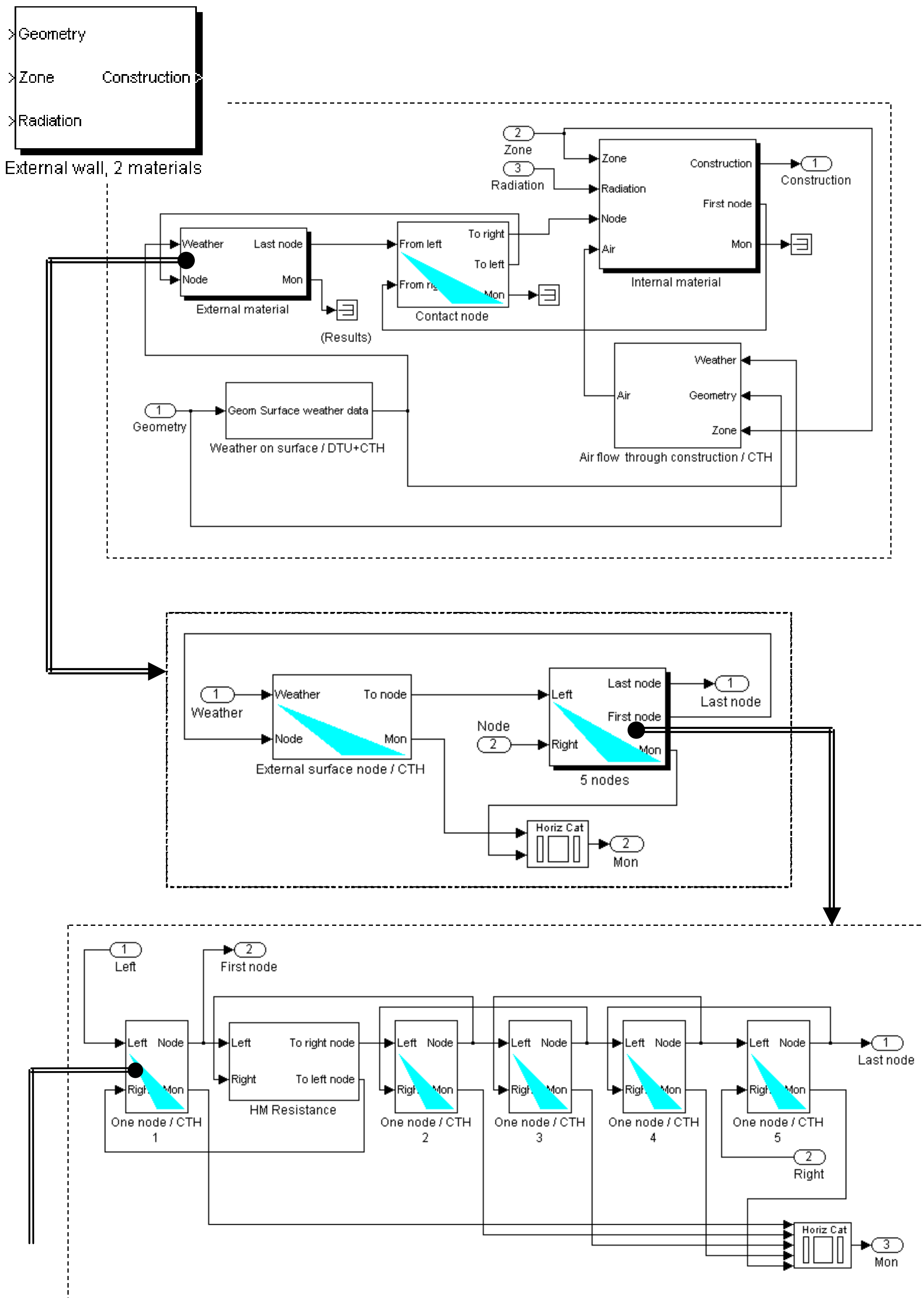

Figure 3.2 Simulink model of the external wall from Figure 3.1 with sub-models. ‘Helpers’ blocks.

3.1.1 External surface node

The ‘External surface node’ represents the external wall surface which is exposed to the convective heat and water vapor exchange with the outdoors air, incident solar radiation, long-wave radiation, air flow and rain, Figure 3.1.

The thermal (vapor, liquid) resistance between the node and the surface of the volume (corresponds to the total thickness *d*) are defined as

$$R = \frac{d}{\lambda}, \; R_p = \frac{d}{\delta_p}, \; R_s = \frac{d}{\lambda_{m,l}} \tag{55}$$

The node position is denoted with an index *i*, and the position of the next one with *i+1*. *n* and *n+1* denote previous and corresponding time steps.

Heat and moisture balance equations in discretized form read:

$$\begin{aligned} \frac{T_i^{n+1} - T_i^n}{\Delta t} = \frac{1}{c_p^n \cdot \rho_s \cdot d} \cdot \Bigg\{ & \left[h_c \cdot \left(T_{air,ext} - T_i\right) + \frac{T_{i+1} - T_i}{R_{i+1} + R_i} \right] \ldots \\ & - h_{e} \cdot \left[\beta_p \cdot \left(p_{v,air,ext} - p_{v,i}\right) + \frac{p_{v,i+1} - p_{v,i}}{R_{p,i+1} + R_{p,i}} \right] \Bigg\}^n \ldots \\ & + g_{rain} c_{p,l} \left(T_{air,ext} - T_i\right)^n + q_{rad,ext} + \begin{cases} g_{air} \cdot c_{p,air} \cdot \left(T_{air,ext} - T_i\right)^n, & g_{air} > 0 \\ g_{air} \cdot c_{p,air} \cdot \left(T_i - T_{i+1}\right)^n, & g_{air} < 0 \end{cases} \end{aligned} \tag{56}$$

$$\begin{aligned} \frac{w_i^{n+1} - w_i^n}{\Delta t} = \frac{1}{d} \cdot \Bigg\{ & \left[\beta_p \cdot \left(p_{v,air,ext} - p_{v,i}\right) + \frac{p_{v,i+1} - p_{v,i}}{R_{p,i+1} + R_{p,i}} \right] - \frac{s_{i+1} - s_i}{R_{s,i+1} + R_{s,i}} \Bigg\}^n \ldots \\ & + g_{rain} + \begin{cases} 6.21 \cdot 10^{-6} \cdot g_{air} \cdot \left(p_{v,air,ext} - p_{v,i}\right)^n, & g_{air} > 0 \\ 6.21 \cdot 10^{-6} \cdot g_{air} \cdot \left(p_{v,i} - p_{v,i+1}\right)^n, & g_{air} < 0 \end{cases} \end{aligned} \tag{57}$$

3.1.2 Internal (one) node

The ‘One node’ block represents one layer (one control volume) of a certain material in the wall construction. It calculates the temperature and moisture content of the node placed in the middle of the layer, accounting for the heat, moisture and air loads, Figure 3.1.

The thermal (vapor, liquid) resistance between the node and the surface of the volume (corresponding to one half of the total thickness d) are defined as

$$R = \frac{d/2}{\lambda}, \; R_p = \frac{d/2}{\delta_p}, \; R_s = \frac{d/2}{\lambda_{m,l}} \tag{58}$$

The specified node position is denoted with an index *i*, and positions of a preceding and a following ones are denoted with *i-1* and *i+1* respectively.

The heat and moisture balance equations in discretized form read:

$$\begin{aligned} \frac{T_i^{n+1} - T_i^n}{\Delta t} = \frac{1}{c_p^n \cdot \rho_s \cdot d} \cdot \Bigg[& \left(\frac{T_{i-j} - T_i}{R_{i-1} + R_i} + \frac{T_{i+1} - T_i}{R_{i+1} + R_i} \right) \ldots \\ & - h_{e} \cdot \left(\frac{p_{v,i-1} - p_{v,i}}{R_{p,i-1} + R_{p,i}} + \frac{p_{v,i+1} - p_{v,i}}{R_{p,i+1} + R_{p,i}} \right) \Bigg]^n \\ & + \begin{cases} g_{air} \cdot c_{p,air} \cdot (T_{i-1} - T_i)^n, & g_{air} > 0 \\ g_{air} \cdot c_{p,air} \cdot (T_i - T_{i+1})^n, & g_{air} < 0 \end{cases} \end{aligned} \tag{59}$$

$$\begin{aligned} \frac{w_i^{n+1} - w_i^n}{\Delta t} = \frac{1}{d} \cdot \Bigg[& \left(\frac{p_{v,i-1} - p_{v,i}}{R_{p,i-1} + R_{p,i}} + \frac{p_{v,i+1} - p_{v,i}}{R_{p,i+1} + R_{p,i}} \right) - \left(\frac{s_{i-1} - s_i}{R_{s,i-1} + R_{s,i}} + \frac{s_{i+1} - s_i}{R_{s,i+1} + R_{s,i}} \right) \Bigg]^n \ldots \\ & + \begin{cases} 6.21 \cdot 10^{-6} \cdot g_{air} \cdot (p_{v,i-1} - p_{v,i})^n, & g_{air} > 0 \\ 6.21 \cdot 10^{-6} \cdot g_{air} \cdot (p_{v,i} - p_{v,i+1})^n, & g_{air} < 0 \end{cases} \end{aligned} \tag{60}$$

The moisture content of the node is limited to w_{cap} (or w_{sat} depending on which type of sorption isotherm is used for material characterization. See Section 2.1.2)

3.1.3 Internal surface node

The 'Internal surface node' represents the internal wall surface which is exposed to the convective heat and water vapor exchange with the indoor air, transfer of latent heat and air, and long wave radiation exchange with other surfaces.

The thermal (vapor, liquid) resistance between the node and the surface of the volume (corresponding to the total thickness d) are defined with Equation 55.

The heat and moisture balance equations in discretized form read:

$$\begin{aligned} \frac{T_i^{n+1} - T_i^n}{\Delta t} = \frac{1}{c_p^n \cdot \rho_s \cdot d} \cdot \Bigg\{ & \left[h_c \cdot (T_{air,int} - T_i) + \frac{T_{i-1} - T}{R_{i-1} + R_i} \right] \ldots \\ & - h_{e} \cdot \left[\beta_p \cdot (p_{v,air,int} - p_{v,i}) + \frac{p_{v,i-1} - p_{v,i}}{R_{p,i-1} + R_{p,i}} \right] \Bigg\}^n \\ & + q_{rad,int} + \begin{cases} g_{air} \cdot c_{p,air} \cdot (T_{air,int} - T_i)^n, & g_{air} < 0 \\ g_{air} \cdot c_{p,air} \cdot (T_i - T_{i-1})^n, & g_{air} > 0 \end{cases} \end{aligned} \tag{61}$$

$$\frac{w_i^{n+1} - w_i^n}{\Delta t} = \frac{1}{d} \cdot \left\{ \left[\beta_p \cdot \left(p_{air,int} - p_{v,i} \right) + \frac{p_{v,i-1} - p_{v,i}}{R_{p,i-1} + R_{p,i}} \right] - \frac{s_{i-1} - s_i}{R_{s,i-1} + R_{s,i}} \right\}^n \ldots$$
$$+ \begin{cases} 6.21 \cdot 10^{-6} \cdot g_{air} \cdot \left(p_{v,air,int} - p_{v,i} \right)^n, & g_{air} < 0 \\ 6.21 \cdot 10^{-6} \cdot g_{air} \cdot \left(p_{v,i} - p_{v,i-1} \right)^n, & g_{air} > 0 \end{cases} \tag{62}$$

3.1.4 Contact node

The ‘Contact node’ block represents a contact surface between two materials in a wall construction, Figure 3.1. It calculates the temperature and moisture contents at the contact surface, taking into account heat and moisture fluxes from both sides.

The ‘Contact node’ is a ‘dual’ node whose left part is made of the left-side material, and the right part of the right-side material. Unlike with the ‘One node” block model, ‘lumped thermal and moisture capacities of the contact node are not localized in the middle of the node – this position is specified by the thickness of the left and right part.

The thermal (vapor, liquid) resistance between the contact node and the surface of the preceding volume (corresponds to the total thickness d_{left}) are defined as

$$R_{left} = \frac{d_{left}}{\lambda_{left}}, \; R_{p,left} = \frac{d_{left}}{\delta_{p,left}}, \; R_{s,left} = \frac{d_{left}}{\lambda_{m,l,left}} \tag{63}$$

The thermal (vapor, liquid) resistance between the contact node and the surface of the following volume (corresponds to the total thickness d_{right}) are defined in the same manner. Thermal capacities of the left and right partitions are:

$$C_{left} = d_{left} \cdot c_{p,left} \cdot \rho_{s,left}, \qquad C_{right} = d_{right} \cdot c_{p,right} \cdot \rho_{s,right} \tag{64}$$

The heat and moisture balance for this “dual” node read:

$$\frac{T_i^{n+1} - T_i^n}{\Delta t} = \frac{1}{(C_{left} + C_{right})^n} \cdot \left[\frac{T_{i-1} - T_i}{R_{i-1} + R_{i,left}} + \frac{T_{i+1} - T_i}{R_{i+1} + R_{i,right}} \ldots \right.$$
$$\left. - h_{e} \cdot \left(\frac{p_{v,i-1} - p_{v,i}}{R_{p,i-1} + R_{p,i,left}} + \frac{p_{v,i+1} - p_{v,i}}{R_{p,i+1} + R_{p,i,right}} \right) \right]^n$$
$$+ \begin{cases} g_{air} \cdot c_{p,air} \cdot \left(T_{i-1} - T_i \right)^n, & g_{air} > 0 \\ g_{air} \cdot c_{p,air} \cdot \left(T_i - T_{i+1} \right)^n, & g_{air} < 0 \end{cases} \tag{65}$$

$$d_{left}\frac{w_{i,left}^{n+1}-w_{i,left}^{n}}{\Delta t}+d_{right}\frac{w_{i,right}^{n+1}-w_{i,right}^{n}}{\Delta t}\ldots$$
$$=\left[\left(\frac{p_{v,i-1}-p_{v,i}}{R_{p,i-1}+R_{p,i,left}}+\frac{p_{v,i+1}-p_{v,i}}{R_{p,i+1}+R_{p,i,right}}\right)\ldots\right.$$
$$\left.-\left(\frac{s_{i-1}-s_{i}}{R_{s,i-1}+R_{s,i,left}}+\frac{s_{i+1}-s_{i}}{R_{s,i+1}+R_{s,i,right}}\right)\right]^{n}\ldots \tag{66}$$
$$+\begin{cases}6.21\cdot 10^{-6}\cdot g_{air}\cdot\left(p_{v,i-1}-p_{v,i}\right)^{n}, & g_{air}>0\\ 6.21\cdot 10^{-6}\cdot g_{air}\cdot\left(p_{v,i}-p_{v,i+1}\right)^{n}, & g_{air}<0\end{cases}$$

Using the expression for the moisture capacity, Equation 20, the following relation can be established, getting the relative humidity (for example) as the common physical parameter:

$$d_{left}\frac{w_{i,left}^{n+1}-w_{i,left}^{n}}{\Delta t}+d_{right}\frac{w_{i,right}^{n+1}-w_{i,right}^{n}}{\Delta t}=\ldots$$
$$=(\,d_{left}\cdot\xi_{left}+d_{right}\cdot\xi_{right}\,)\cdot\frac{\phi_{i}^{n+1}-\phi_{i}^{n}}{\Delta t} \tag{67}$$

3.1.5 Air flow thorough the wall

The 'Air flow through the wall' block calculates the net volumetric airflow through the construction, Figure 3.1. This airflow is modeled by Equation 35 (and divided by the wall area), from section 2.3.1. The corresponding mass flow rate is then calculated by Equation 6, and implemented as a pre-calculated value in Equations 9 and 12. Thus, the airflow rate, q_{air} or g_{air}, is constant throughout the whole structure, allowing for variations in time.

3.1.6 Heat and moisture resistances in the wall

The 'Resistance' block represents an additional resistance R, which corresponds to either a heat, a vapor or a liquid resistances (R, R_p, R_s), Figure 3.1. These resistances are simply added to the resistances of the neighboring nodes, Figure 3.1. For example, the liquid flow resistance for the node on the left is changed to:

$$R_l^{*}=R_l+R \tag{68}$$

and for the node on the right to:

$$R_r^* = R_r + R \tag{69}$$

3.1.7 Material data

The following material data are relevant for the model:

Density of the dry material
Open porosity
Specific heat capacity of the dry material
Thermal conductivity, according Equation 17
Sorption isotherm, according Equation 18
Moisture capacity, according Equation 20
Water vapor permeability, according Equation 12
Liquid water conductivity, according Equation 11
Air permeability (necessary when it is used for the airflow calculations)
Absorptivity for solar radiation
Emissivity
Transmittance

Data can be given as constants, functions or tables of values. Figure 3.3. The selected Simulink model represents the block ‘Material data’, which reads material properties from a material data base. Such block is an integrated part of ‘External surface node’, ‘Internal (one) node’, ‘Internal surface node’ and ‘Contact node’ (Sections 3.1.1-3.1.4).

Material data are stored in a material database which is in the form of structures. Structures are multidimensional Matlab arrays with ‘data containers’ called fields. Each field has a certain name and can contain either a text, a scalar, an array or a matrix. Here is an example:

```
CTHmaterial(2)=struct(...
    'index',2,...
    'name','Plaster',...
    'dry_density',790,...
    'lambda_dry',0.2,...
    'lambda_T',0,...
    'lambda_W',0.0045,...
```

Each material from the library is described by the same set of data, but with the different order number – ‘index’ (see above list). An overview of the reserved field names is given in Rode et. al. (2002a). Any other material property can be added, but with another name. Any user can change and extend the contents of the material library.

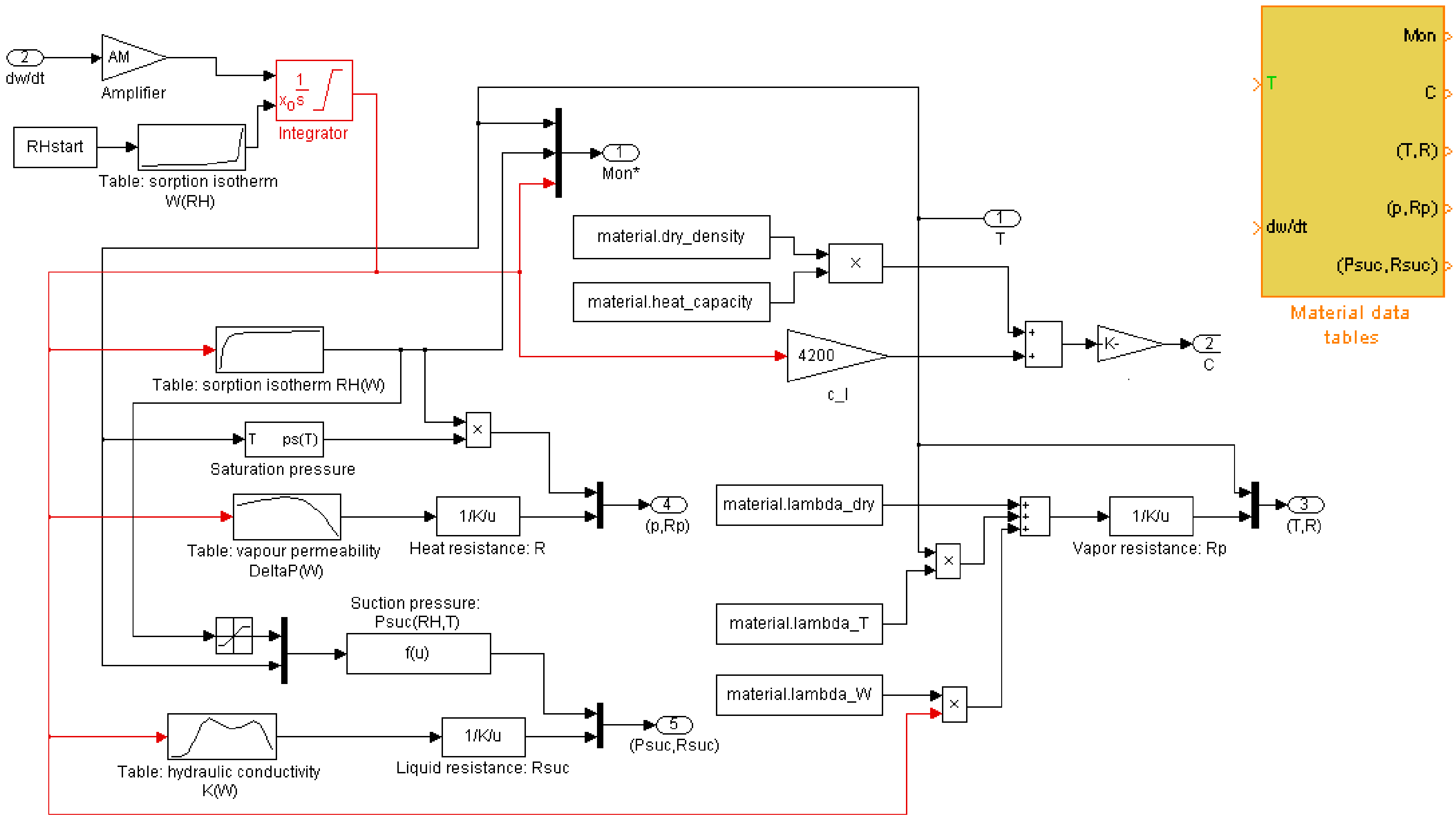

Figure 3.3 HAM-Tools block “Material data”.

3.2 Internal air-zone

The internal air zone is regarded as the air-zone enclosed by the building envelope. It can be any indoor-air partition, like a room, an attic, etc., or a ventilated cavity inside a wall construction. A numerical model of the air-zone is based on the governing equations from Section 2.3; the corresponding Simulink model is designed as one block and placed in the 'Zone' library. Both the numerical model and the Simulink model of the 'Zone' block are presented in Figure 3.4.

Governing equations for the heat, air and moisture balance of the air zone in discretized form read:

$$C_H \cdot \frac{T^{n+1}_{air,int} - T^{n}_{air,int}}{\Delta t} = Q^{n}_{construction} + Q^{n}_{vent} + \Phi^{n}_{c} \tag{70}$$

$$C_M \cdot \frac{p^{n+1}_{v,air,int} - p^{n}_{v,air,int}}{\Delta t} = \left(M_{constructions} + M_{systems} + M_{gains}\right)^{n} \tag{71}$$

$$P^{n}_{air,int} = \frac{\sum\limits_{k=1}^{Sysnr+Snr} Q^{n}_{air,k}}{\sum\limits_{k=1}^{Sysnr+Snr} R_{a,k}} \tag{72}$$

This model is constructed under the assumption that the indoor air is well mixed, and thus it can be represented with one (numerical) node. The other air node that appears in Figure 3.4 is just a fictitious one, coming from the model for the long-wave radiation exchange. This temperature is defined from the mean surface temperature and radiation heat sources and is called the radiative temperature. However, its definition is hidden in Equation 46.

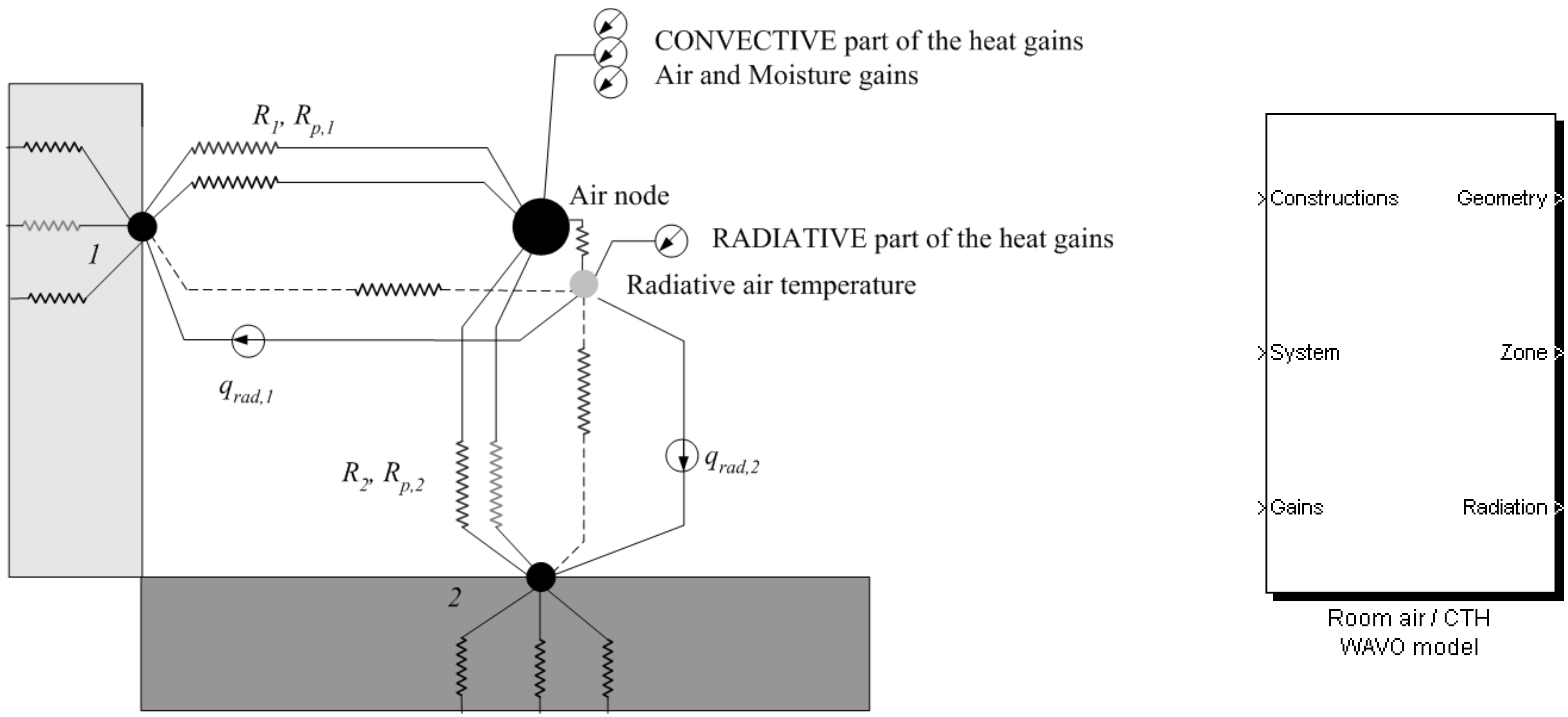

Figure 3.4 Numerical model for the air zone and the Simulink block.

3.3 Environmental conditions

3.3.1 Weather file

The following outdoor climate parameters are relevant for the model:

Air temperature
Dew point temperature
Global radiation on horizontal surface
Diffuse radiation on horizontal surface
Normal direct radiation
Incident long-wave radiation
Wind speed and direction
Total pressure
Rainfall

The data should be on hourly time scale and for the period of one year, but other combinations are also possible. This so called 'Weather' file has a definite structure, which is defined in Rode et.al. (2002a). A block with the corresponding name is available from the 'Helpers' library; it serves to read the data from the file into the Simulink modeling sheet.

3.3.2 Solar radiation model

In addition to the climate parameters, the geographical location of the selected sight should be also known, i.e. its

Latitude
Longitude
Local standard mean time

These parameters enable the calculation of the proper amount of solar and long-wave radiation energy for a specific building side, whose

Tilt and
Orientation

are also known. The whole procedure is incorporated in the block 'Weather on surface', from the 'Helpers' library, which is shown in Figure 3.2. This procedure is designed by the research group from the Technical university of Denmark, and is provided in the International Building Physics Toolbox (IBPT).

3.3.3 Weather on surface

The ‘micro’ climate parameters at a specific building side are defined in the block ‘Weather on surface’. These are:

Direct solar radiation
Diffuse solar radiation
Incident angle of solar radiation
Air temperature
Wind speed
Relative humidity
Long-wave radiation from surroundings
Rain on surface
Air pressure

Data refer to the quantity perpendicular to the surface, like solar radiation and wind, or at the surface, like for example air pressure.

A simple model for wind pressure distribution around the building is also incorporated in this block. The wind pressure is estimated from the wind speed intensity and surface pressure coefficients for the building; the latter depend on the angle at which the wind ‘hits’ the surface. This procedure is given in Sanders (1996), and one example of the model is presented in **Paper III**.

The amount of rain that reaches the building surface, depends on the wind parameters (speed and direction) and on the shape and height of the building. At the moment, there is no model for the rain distribution estimation around the building; these data should be provided from other sources.

3.4 Sources

Heat, air and moisture sources to the zone are defined in accordance with the purpose of the zone and its occupancy. ‘Systems’ and ‘Gains’ tools serve to model a desired HAM load, but also ‘Constructions’ tools. The tools are structured so that either a constant or a variable load can be modeled, with or without a control system. It is also possible to model non-standard components, like integrated HVAC systems. One example is given in **Paper III**, where the heating of the test house is accomplished by a floor heating system, inbuilt in the floor construction.

3.5 Whole building

By combining different tools such as a single-layer wall in a multi-layer wall, a couple of different walls in a zone, several zones in a building, and finally together with climate load and HVAC equipment, it is possible to built the house as a system. Some of the one-zonal systems are presented in **Paper I**, **III** and **V**. A system with two air zones, a dwelling and an adjacent attic, is illustrated in Figure 3.5, (Serkitjis and Sasic, 2004).

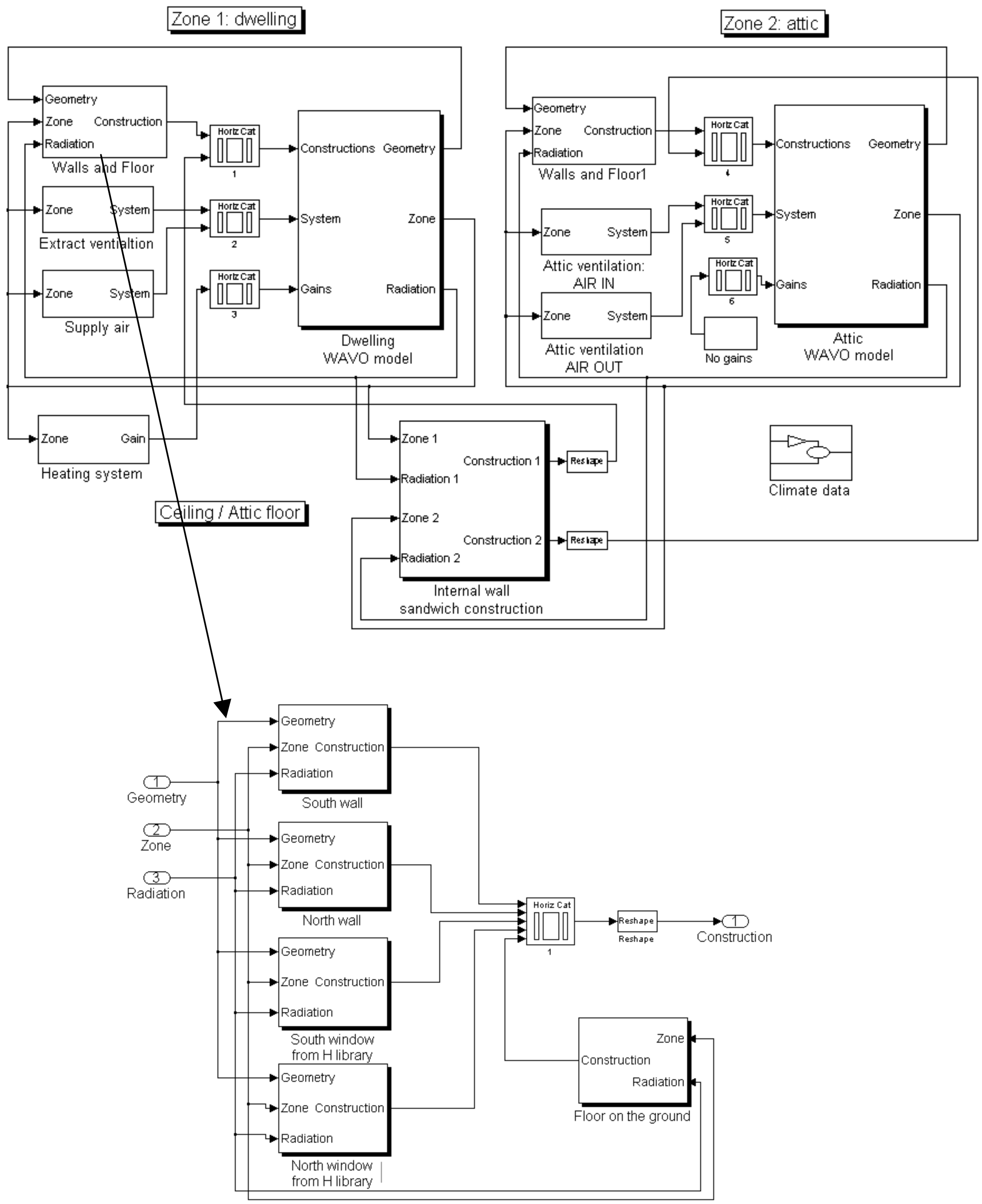

Figure 3.5 A model with two zones.

The (space) position of the wall is defined in the zone. Details like orientation, tilt and area are stored in the 'Geometry array', for each of the attached components. The 'Weather to surface' block, Section 3.3.3, which is included in each of the attached

‘Construction’ blocks, reads the general climate data from the ‘Climate data’ block, and geometry data from the ‘Geometry array’. The general climate data are then processed in accordance with the wall position, and the right amount of solar and long wave radiation, wind speed, wind pressure coefficient and rain are calculated for the concerned wall. For the sake of the simplicity, communication signals from the ‘Climate data’ block to the ‘Construction’ block are hidden on the highest model level.

Besides the ‘Geometry array’, two more signals are defined in the zone: the ‘Zone’ signal, which contains the indoor climate data, and the ‘Radiation’, which contains the long-wave radiation energy that is calculated within the zone.

Input signals to the zone are ‘Constructions’, with the data about HAM states at internal sides of attached walls and windows, ‘Systems’ with HAM states at the inlet of the (ventilation) system and ‘Gains’, with the magnitude of the additional HAM sources.

Figure 3.6 illustrates these and some additional features of the toolbox, in the terms of the network. The presented system consists of three zones: a dwelling, a crawl space and an attic. Zones are connected with each other and with external climate over the ‘attached’ building structure components: walls and windows.

Since HAM-Tools provides one-dimensional calculations in a wall, there is no possibility to simulate two-dimensional effects like thermal bridges. Thus, walls ‘see’ each other only over the zone and there is no coupling between them along the connecting lines. This is indicated by the ‘missing’ corners at places where two walls meet.

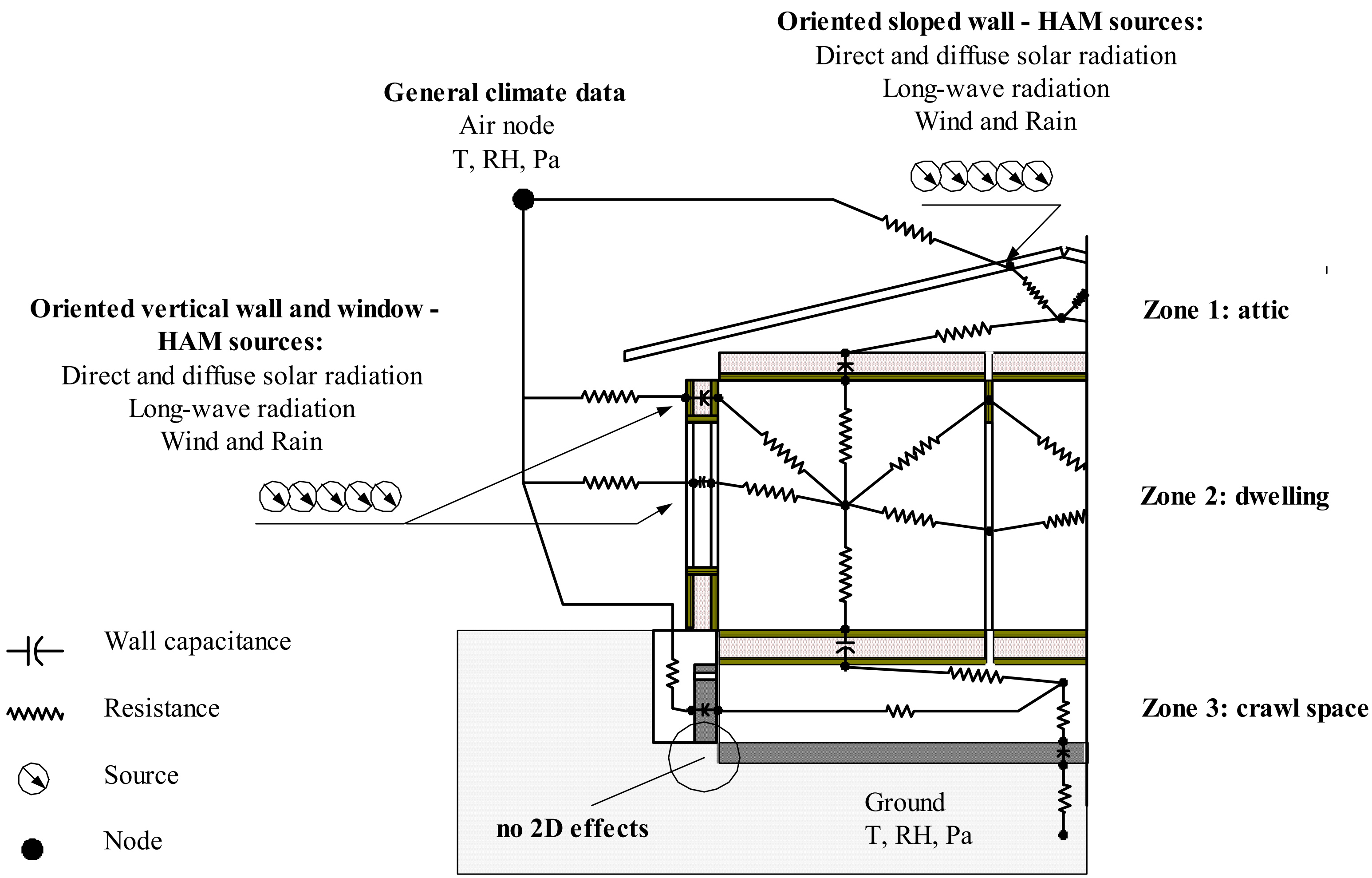

Figure 3.6 Coupling between building enclosure and air zones in terms of networks.

4. SELECTED EXAMPLES OF THE APPLICATION OF THE CODE

4.1 Air transport in and around the building

HAM-Tools provides calculation of the airflow (air infiltration) through the porous wall structure and also the calculation of the air balance for the zone.

4.1.1 Air transport through the wall

When present, the movement of air through a wall (air-filtration) gives the main contribution to the transport of vapor and heat (Equations 9 and 12). Certain wall constructions, such as light-weight walls and constructions with air-cavities, usually give rise to the development of such a flow, which is basically governed by pressure and temperature differences across the construction.

The hygro-thermal situation in the wall with the air filtration present can be completely different from the case without it. For example, in areas with colder climates, an ex-filtration of the warm humid air from the interior can accelerate the occurrence and magnitude of interstitial condensation. In case of the air infiltration, when cold and dry air from exterior goes into the construction, the risk of the interstitial condensation is very small. A calculation example that illustrates this situation is given in **Paper II**, by the HAMSTAD Benchmark number 3. The benchmark deals with a light-weight wall exposed to ex-filtration during 20 days, followed by air infiltration during next 80 days, Figure 4.1. Moisture transfer is caused mainly by the airflow through the layer, but also by the moisture and temperature gradients across the layer. The external side of the wall is vapor tight but air-open.

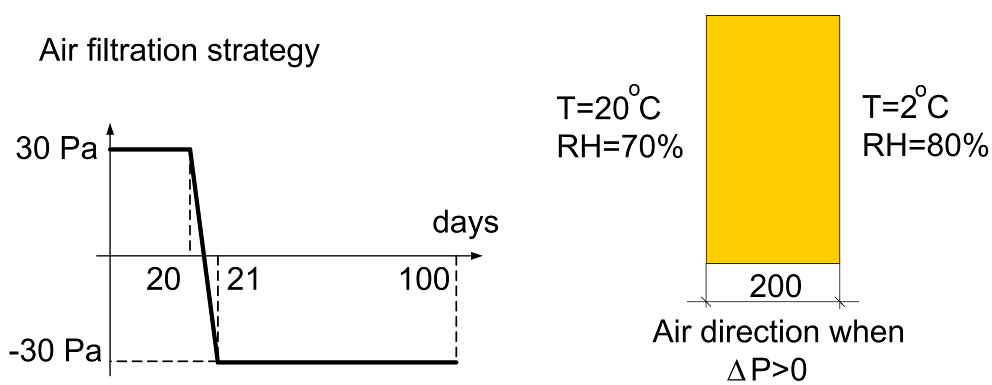

Figure 4.1 Light-weight wall and the air filtration strategy. Benchmark 3, **Paper II**.

Results of the simulation are given in Figure 4.2, in form of the temperature and moisture distribution in time in different sections of the wall. During the period of exfiltration, moisture content in the wall is increased up to 96 %. The wall is dried out during the period of infiltration.

The movement of air inside the wall is much more complex than modeled by HAM-Tools, as an one-dimensional transport process. The more adequate is the two-dimensional (2D) approach (Janssens, 1998; Wang, 2003), but the three-dimensional (3D) probably gives the best prediction. However, as long as the problem can be considered as one-dimensional, HAM-Tools provides a proper representation of the consequences of air filtration.

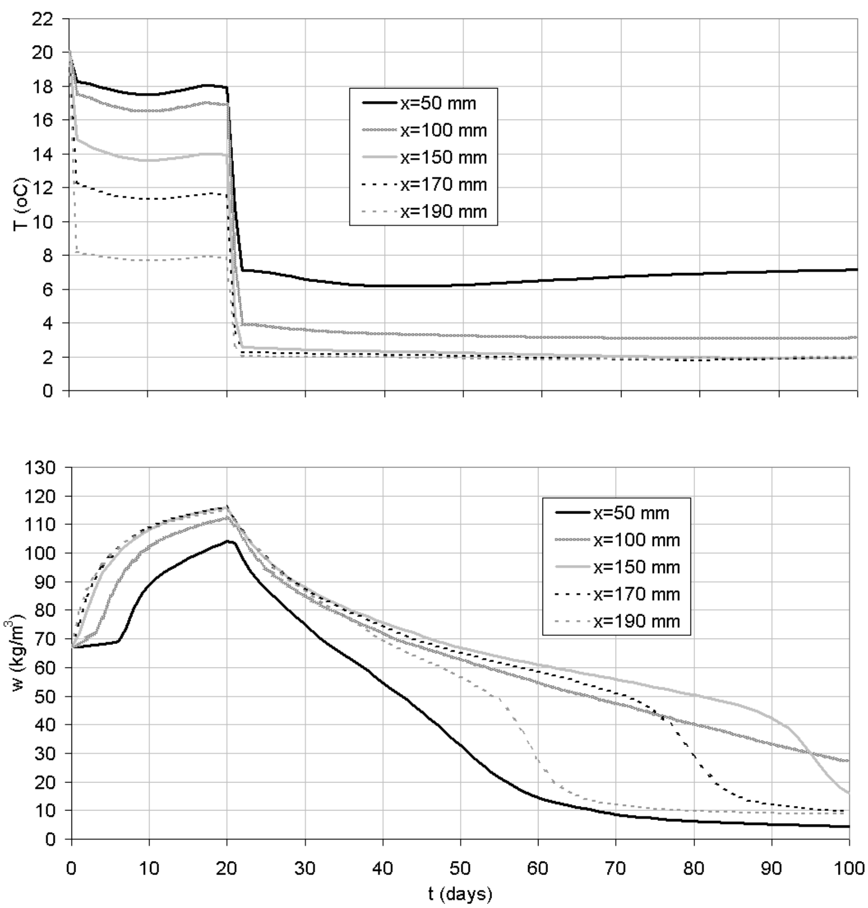

Figure 4.2 Temperature and moisture distribution in time in different wall sections in the presence of air filtration. Results for the HAMSTAD Benchmark 3, **Paper II**, obtained by HAM-Tools.

4.1.2 Air transport through the zone

This is another type of the air flow analyses which can be performed by HAM-Tools. The air comes into or goes out from the zone by means of the ventilation system, or through unintentional openings (cracks, leakages) due to pressure and temperature differences between the indoor and outdoor air. Since ventilation heat losses dominate among total losses for the well insulated building, the air handling and air flow calculations have been an important issue among researchers and practitioners.

Basically, 'System' tools are used for the modeling of the airflow through openings, but 'Construction' tools will also contribute with the part coming from the air filtration. The air flow through openings is modeled in a simplified way, as it is described by Equation 35. The modeling of the inter-zonal flow is also possible.

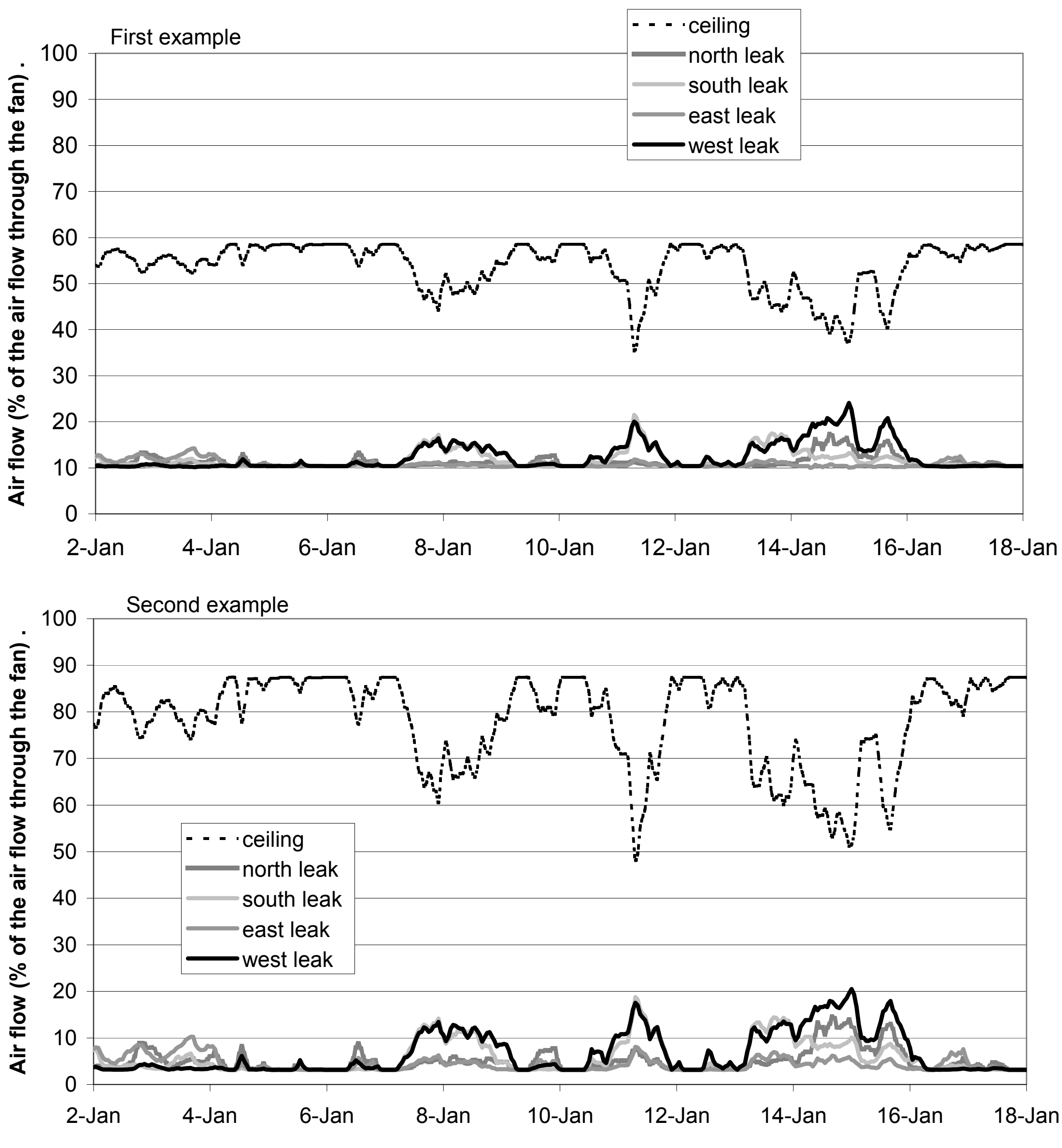

Figure 4.3 Airflow through the building in the presence of air leakages. Flows through dynamic ceiling and air leakages are expressed as percentage of the total (designed) flow. The upper figure shows results for the first case, with 'poor' airflow characteristics of the dynamic ceiling. The Figure below presents results for the second case, with improved flow characteristics.

Recently and for research purposes, special attention is dedicated to the investigation of the air flow through cracks and leakages on building assemblies (some data are summarized in TN AIVC 44, 1998). In wooden constructions, which are common in Sweden, air leakages along the wall assemblies are almost inevitable. The airflow thorough such unintentional openings may influence the functionality of the ventilation system. An example is given in **Paper III**, showing how the functionality of a dynamically insulated wall (ceiling) can be significantly changed in the presence of air leakages on the constructions. Two cases are analyzed. In the first case, the airflow resistance of the dynamic ceiling is of the same order as for the air leakages. Simulation results show that the airflow through the ceiling is maximum 60 % of the designed one, Figure 4.3. In the second case, the airflow characteristics of the ceiling is improved (lower airflow resistance) and the airflow reaches 90% of the designed one. In both cases, the airflow through the dynamic ceiling is decreased when the wind acts, and a significant amount of un-preheated air is drawn into the house.

4.2 Interstitial condensation – moisture transport over the contact surface

Under certain conditions, interstitial condensation takes place inside a construction. It is very important to provide tools for the simulation of such effects, since they contribute to fast deterioration of the structure.

The capillary water transport plays an important role in the redistribution of the condensate that occurs. Generally, if condensation occurs at the contact surface between two capillary active materials, the condensate is redistributed between both. Furthermore, a high capillary activity in combination with high moisture capacity of the material can protect the construction from the condensation. An example is given in the HAMSTAD Benchmark 5, **Paper II**.

If condensation occurs at the contact surface between a capillary active and capillary non-active material, the condensate redistribution can be somewhat different. An example is given in **Paper II** again, Benchmark number 1. The Benchmark deals with an internally insulated roof with a (known) problem of interstitial condensation at the contact surface between load bearing and insulating material, Figure 4.4. The structure is perfectly air tight, and no vapor exchange is possible with the exterior. The applied external climatic load corresponds to the North-European conditions, while the internal climate is the common one in dwellings. The simulation covers five years.

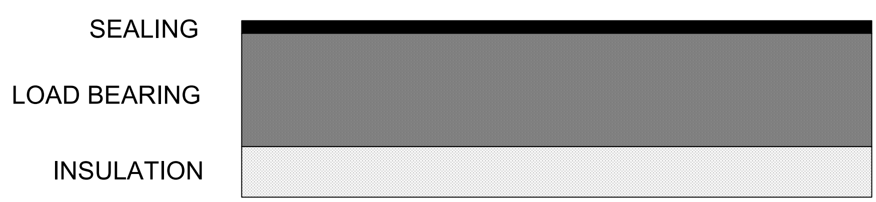

Figure 4.4 Internally insulated roof. Benchmark 1, **Paper II**.

In the beginning, the load bearing material is completely wet. The drying starts already in the first year, in the spring time, as the solar radiation intensity increases. In winter, a reverse process occurs - vapor from the dwelling diffuses into the construction and condensates in the colder parts.

Since the load bearing material is colder and capillary active, it is to be expected that the condensate will be ‘pushed’ into this part. However, in the beginning of the first year, the load bearing layer is almost completely saturated with moisture, and apart from some small amount of the condensate which is redistributed on that side, the rest is passed to the insulation, Figure 4.5

In situations like this, i.e. when the coupling between capillary active and capillary non-active material is considered, and the interstitial condensation occurs at the contact surface, it is necessary to use a special coupling tool - the ‘Contact node’ (section 3.1.4) and to refine the mesh extremely at the contact surface. Otherwise, the redistribution of the condensate in the insulating material can be missed.

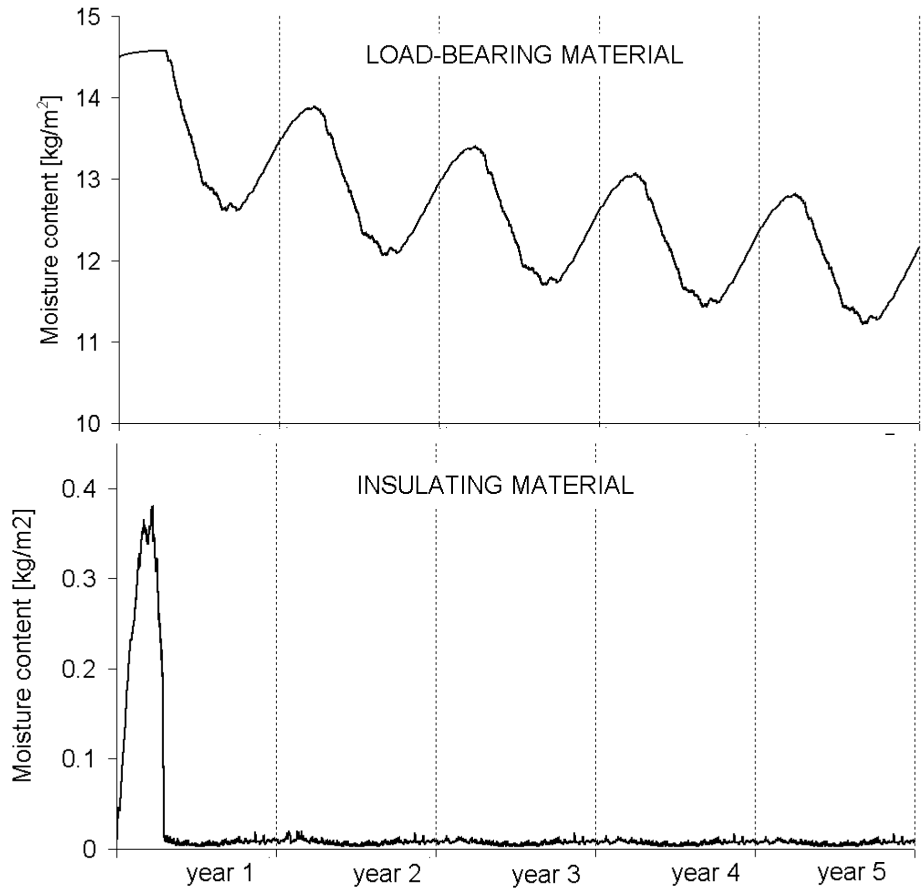

Figure 4.5 Moisture content in load-bearing material (upper figure) and insulation (lower figure), expressed in kg/m^2, during five years. Simulation results for the HAMSTAD Benchmark 1, obtained by HAM-Tools.

4.3 Rapid moisture transport through porous material

Moisture transport that takes place at high moisture levels in materials is also a common process. A few examples can be mentioned: wetting and drying of a façade (Benchmark number 4, **Paper III**), water transport through the ground, or in special applications, such as the storage of the nuclear waste (Claesson et. al. , 2003). A capillary water transport is then a dominant way of the moisture transport through the material.

When compared to heat transport, moisture transport is generally a slow process. For example, 'Cup' experiments take weeks or months until the steady-state is reached, (see for example Broken, 1998). But there are materials that transport moisture rapidly at high moisture levels. Thus, when a specimen of such material is immersed into water, one can clearly see the penetration of the water front (similar to the sponge effect). Such materials are classified as 'low-hygroscopic' but 'highly capillary active' – they have small moisture capacities, but very high coefficients for the liquid moisture transport. Bricks are the main representatives.

Simulations of the rapid moisture transfer through porous media may encounter numerical problems, which are discussed in **Paper IV**. The problem is localized at the 'wetting front' – the boundary that appears between the already wet partition of the material and the one which should be wetted. Very strong moisture flow gradients may appear at the wetting front: the hydraulic conductivity in the partition saturated with water can be by several orders of magnitude larger than in the dry region. In order to 'catch' the moving front, it is known that the numerical mesh should be very refined around it. Since the front moves throughout the whole calculation domain, it implies that the mesh should be fine in the whole domain or be possible to be refined at the moment when the wetting starts. Otherwise, the solution can be far from reality.

The 'moving' front is a well-known problem in numerical modeling and the related literature treats it by using the so-called auto-adaptive mesh – a mesh that 'follows' the front and keeps the refinement only around it, (see for example Fletcher, 1987). There are not many computational codes for building physics applications that use the auto-adaptive mesh refining technique, even if it was proved to be very efficient for this type of problems (Roels, 2000). The majority of the codes work with stationary mesh, and in that case, it is not economical to keep the mesh fine all the time.

As it is analyzed in **Paper IV**, the problem that appears in the numerical domain is actually a consequence of the modeling – the estimation of the interface liquid conductivity between the wet and the dry partition. Three estimation methods are analyzed: harmonic, linear and integral averaging. Two theoretical suction experiments are simulated. In the first experiment, the moisture transport properties of the material are modeled to represent the ones of a common brick: the material is non-hygroscopic, but highly capillary active. It is shown that the harmonic method drastically underestimates the moisture flow over the wetting boundary, and as a consequence of that, a solution which is far from reality, is produced. The other two methods, the linear one and the integral one, are able to produce an accurate solution for the case treated, Figure 4.6. However, if the mesh is not sufficiently refined, the linear method overestimates the flow, and the solution based on this method can differ significantly from the accurate one. The integral method gives the realistic solution already with the coarse mesh. Even with the

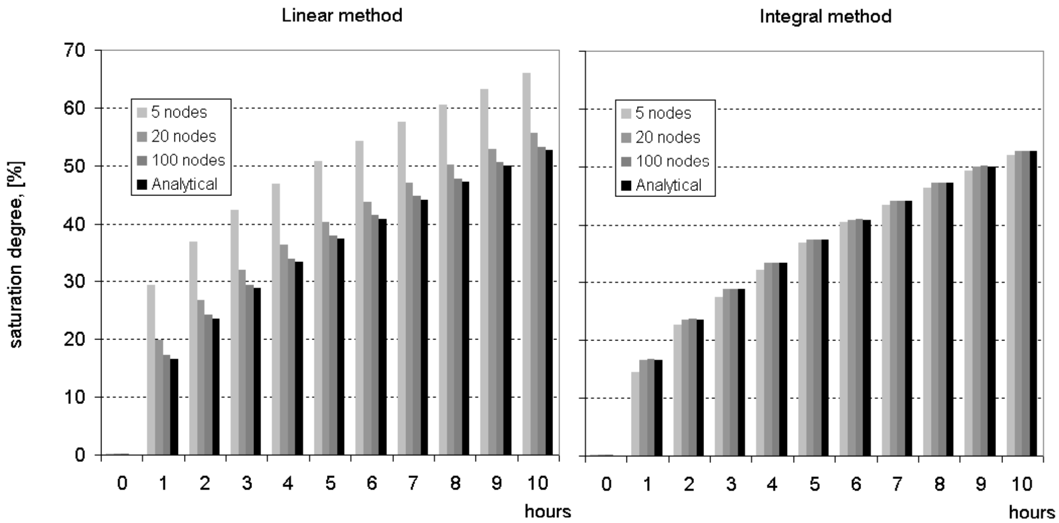

Figure 4.6 Saturation degree of the sample for the first case. Study of the different averaging techniques and different mesh refinement.

moderate mesh refinement, the solution obtained with the integral method converges rapidly to the accurate one.

In the second experiment, only the hydraulic conductivity of the sample is changed so that the material is capillary active also in the unsaturated region. By this, the moisture flow gradient over the wetting front is decreased and an 'easier' numerical problem is generated. Solutions obtained by each of the three methods treated are similar to the ones from the previous case, Figure 4.7. However, the difficulties and discrepancies are not so pronounced.

It is shown that it is possible to produce an accurate solution for the problem of the 'moving boundary' using the stationary mesh, by choosing the proper estimation method for the interface liquid conductivity. The integral method appears to be the most correct one for the problems of rapid moisture transfer under isothermal conditions. The application of this method for non-isothermal moisture transport problems is to be further investigated.

The tools for linear and integral estimation of interface moisture conductivity are provided in the extended version of HAM-Tools.

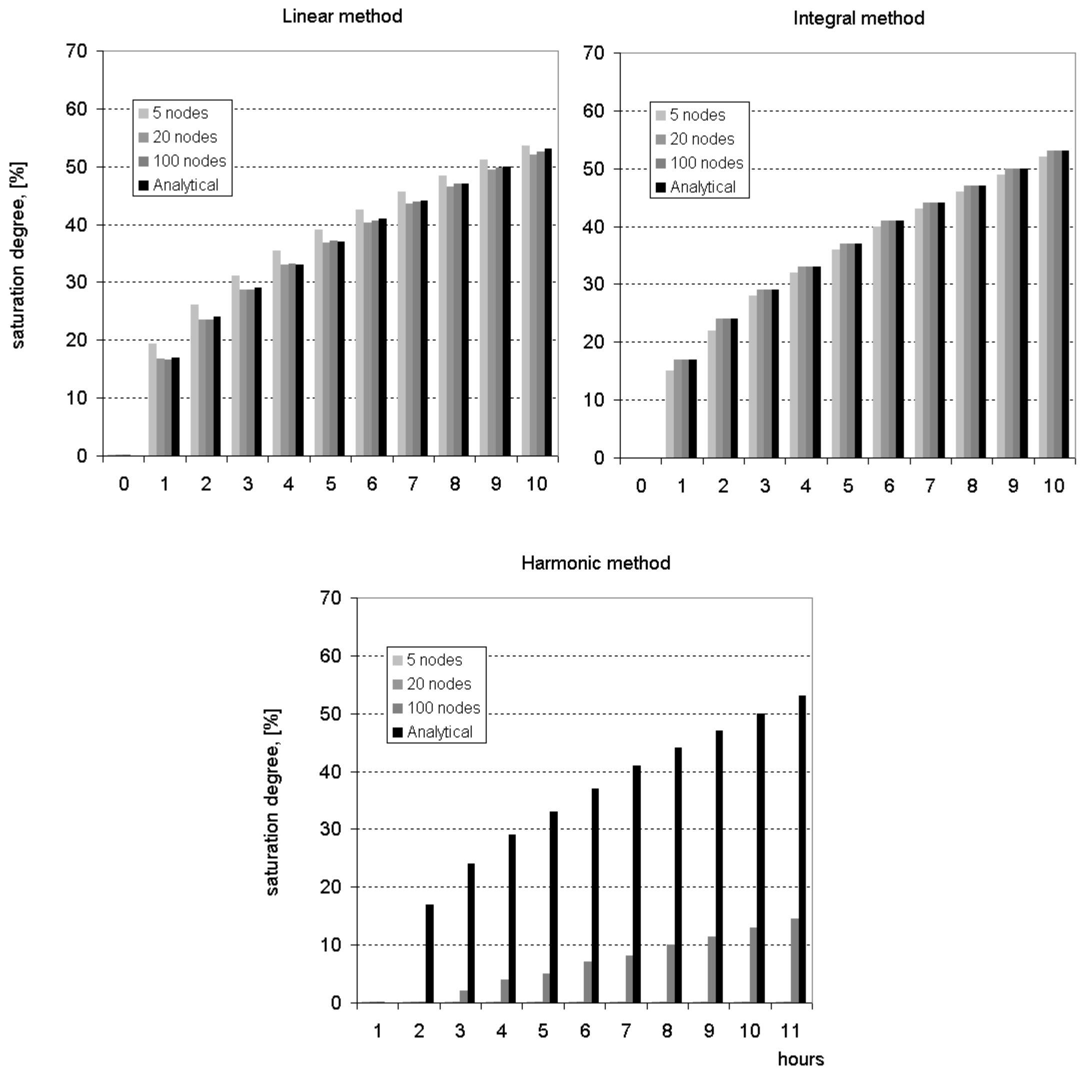

Figure 4.7 Saturation degree of the sample for the second case.

5. VALIDATION OF THE HAM-Tools

As it is discussed in the introductory chapter of this work, one of the tendencies in code development is the code certification, and the most important part of it is the validation test.

Basically, the code can be validated in one of the following ways:

- Analytical validation.
- Comparison with other codes.
- Empirical validation.

Since these methods are different, the code validation using one of them does not guarantee that the code can be validated using other methods.

HAM-Tools ‘Wall’ was validated by the first two methods. The model for a whole building, composed from the standard HAM-Tools blocks, was validated by the third method. Results are summarized hereafter.

5.1 Analytical validation

Analytical validation represents the most reliable test, because the mathematical solution to the problem exists and a divergence from the solution can be exactly evaluated. The shortcoming of such validation is that the solution exists only for simpler, more theoretical cases. However, this type of validation is useful in the first phase of the code development, in order to ensure, for example, that the basic balances are satisfied.

In the draft of the new European standard ‘Hygrothermal performance of building components and building elements – Assessment of moisture transfer by numerical solution’ (CEN/TC 89 WC 29.3), a benchmark with the analytical solution is provided for the code validation. The problem deals with combined heat and moisture transfer in a semi-infinite homogeneous wall. In the beginning, the wall is in equilibrium with a constant surrounding climate. At a certain moment the temperature and relative humidity undergoes a step change. The task is to calculate temperature and moisture profiles at different time steps after this change. The reference analytical solution (solid black line), the band of acceptance (dotted lines) and the solution provided with the HAM-Tools ‘Wall’ block (with circular marker) are presented in Figure 5.1.

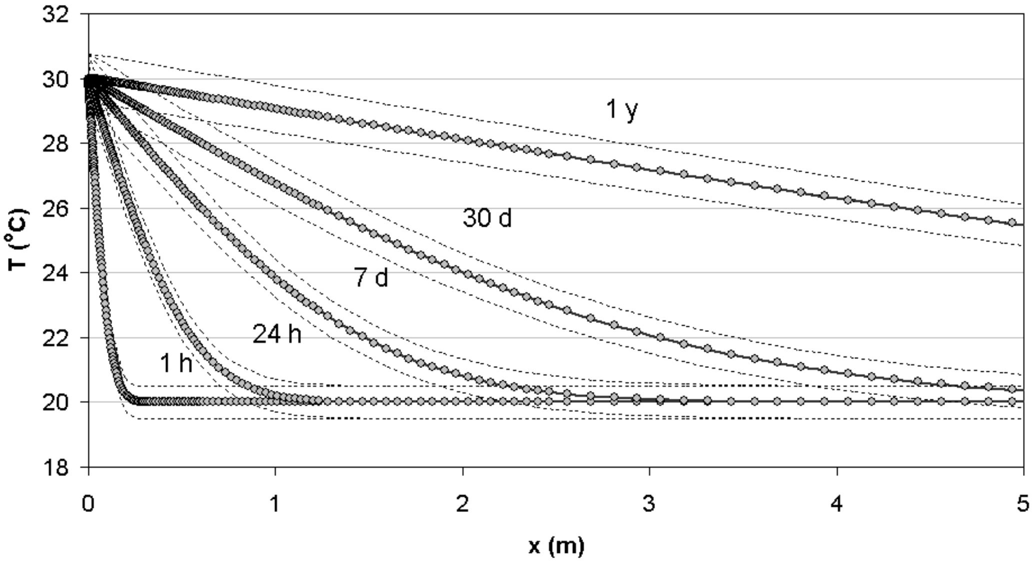

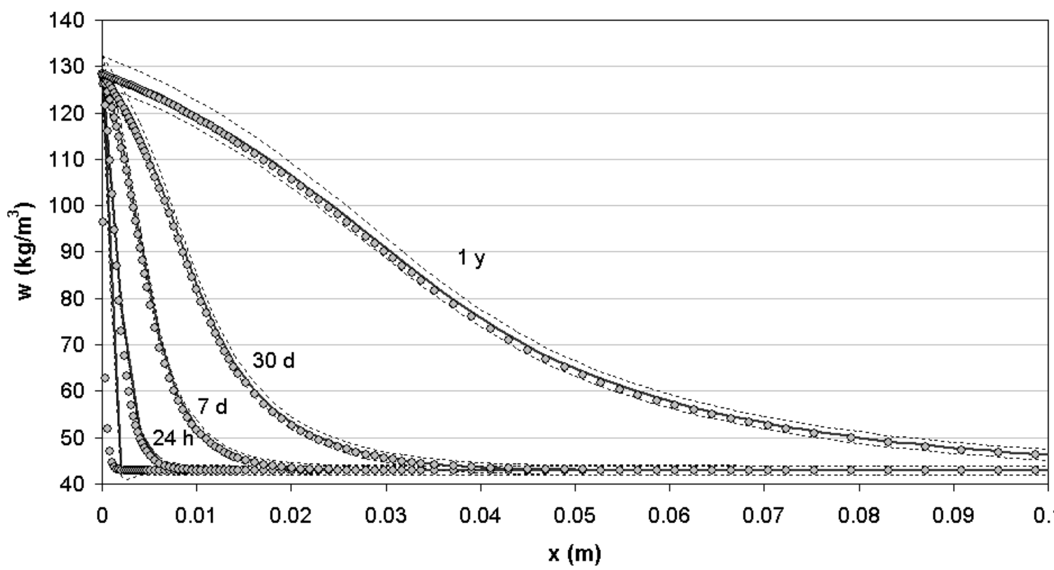

Figure 5.1 Analytical verification. The moisture and temperature distribution at 1h, 24h, 7 days, 30 day and 1 year. The solid black line is the analytical solution; dotted lines show the interval –2.5% and +2.5%. The line with circular marker is the solution by the HAM-Tools.

5.2 Comparison with other codes

When a code is validated against other codes, it means that the code produces as accurate solutions as other ones. This validation is especially convincing against already well-established (reliable and validated) codes.

In the second part of the HAMSTAD project (see also Section 1.2.3), the validation tests of this kind were performed. Some prerequisites were stated for all participants:

- Models are based on the same HAM theory, defined in Hagentoft (2002).

- Same input data are implemented in calculations (e.g. material properties and climate data).

- Exercises represent complex cases, for which analytical solutions are not known, (except for Benchmark number 2).

The outlines of five HAMSTAD benchmarks are presented in **Paper II**. They include the following phenomena:

Benchmark 1: Interstitial condensation at the contact surface between two materials (some details in Section 4.2).
Benchmark 2: Isothermal moisture diffusion (Analytical case).

Benchmark 3: Heat and moisture transfer in the presence of the air convection (some details in Section 4.1.1).
Benchmark 4: Response analyses during subsequent wetting and drying of the wall.
Benchmark 5: Moisture redistribution in highly capillary active materials.

Up to seven transient temperature and moisture solutions for each of the five benchmarks have been obtained. Due to nonlinearity and coupling of the phenomena, the analytical solution exists only for a simple, decoupled case. For this case, differences between numerical and analytical solutions were exactly evaluated. For the remaining cases, correct solutions are not known, but only the approximate ones. There is no certainty that the average of all numerical solutions is the correct one. However, it is reasonable to assume that the correct solution lies close to those that show good agreement.

In order to define a consensus solution, different levels of evaluation were used:

- Level 1: models produced results without divergence, in the physically relevant range.

- Level 2: detailed comparison of temperature and moisture profiles at certain time-steps and certain positions, insuring the same trend and response.

- Level 3: results showed the same average trend in time which can be graphically or numerically evaluated; for example, the average of all obtained results and the maximum and minimum threshold were statistically defined, and then the band of acceptance calculated.

Details about assessment methods are to be found in Hagentoft et.al. (2004). Illustrations of the assessment Level 2 and 3 are given in Figure 5.2.

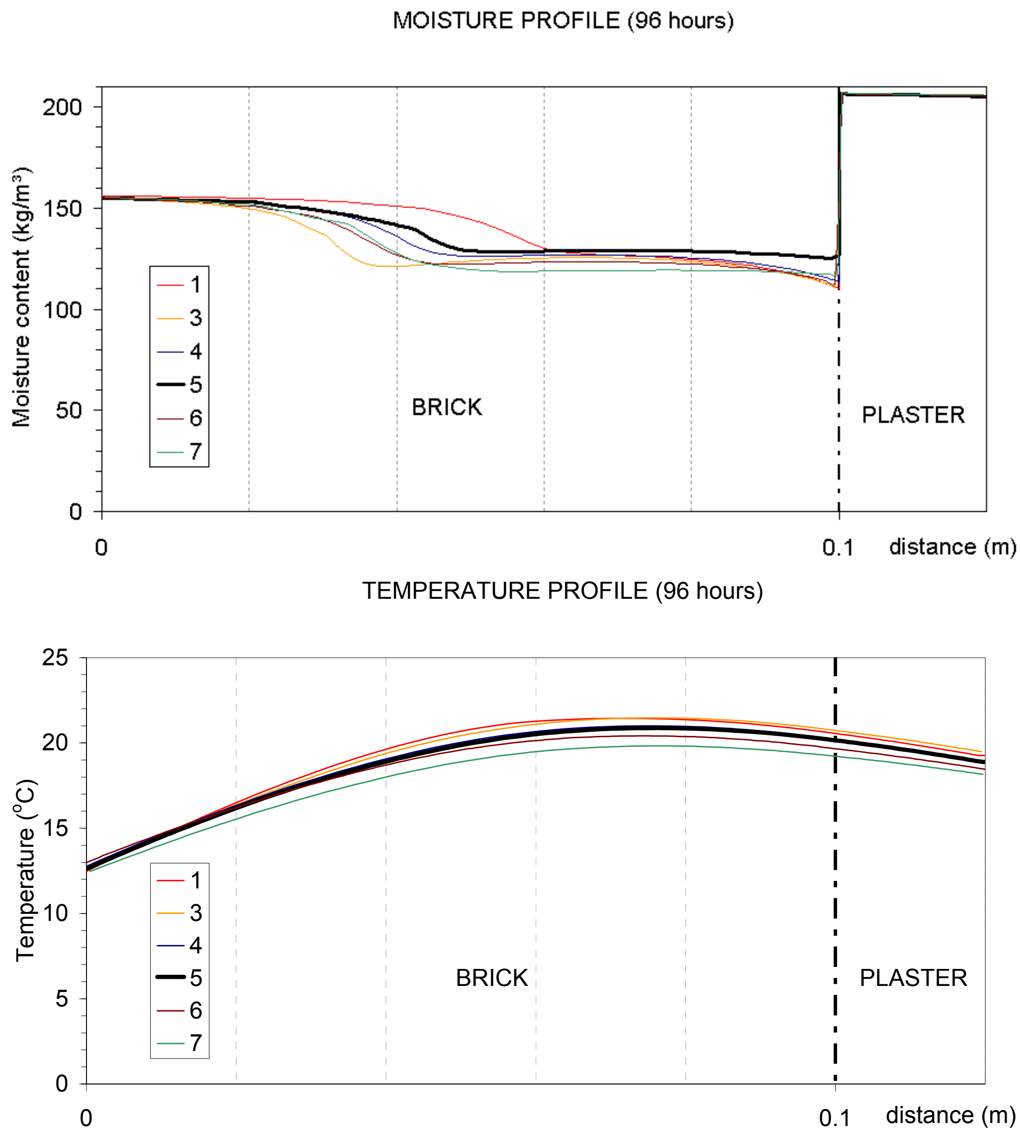

Figure 5.2 Results for the HAMSTAD Benchmark 4 'Response analyses'. Moisture content and temperature distributions through the wall after 96 hours, preceded by three rain-wetting periods and two solar-radiation drying periods. Solution number 5 is the solution obtained with the HAM-Tools 'Wall' block. The agreement between different solutions is good, but one can observe differences in the treatment of the wetting processes.

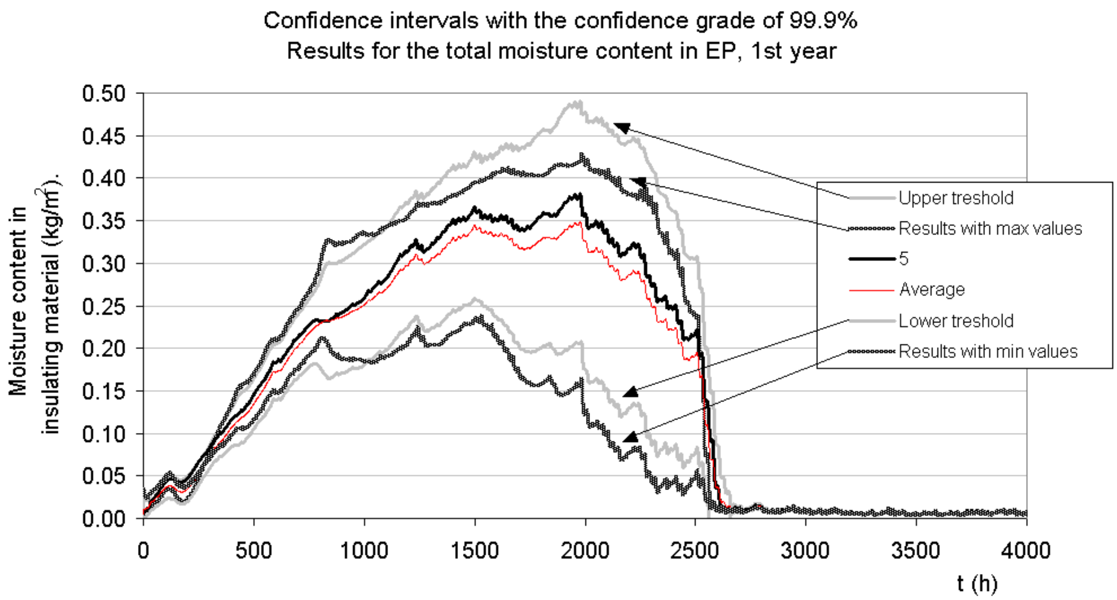

Figure 5.3 Results for the HAMSTAD Benchmark 1. The band of acceptance for total moisture content in the insulating material during the first year, with the confidence interval of 99.9%. Solution number 5 is the solution obtained with HAM-Tools 'Wall' block.

5.3 Empirical validation

Empirical validation represents the validation against measurements, exemplifying to what extent the code can predict the reality. Because of that, this method is highly ranked among code developers and users.

For code developers, empirical validation is not an easy task. A lot of uncertainties can be introduced from the implemented theory, on one side, and from measurements, on the other. A certain theory is valid under certain assumptions, which are inbuilt into the code. Therefore, only the projection of the reality and not the reality itself can be studied. It is important to select the task according to the code capabilities. Then, the empirical validation acts as a proof that the code is capable of representing the selected real model in a credible way, compensating at the same time errors that resulted from the simplification of the problem. Extending the code application beyond the 'validity' domain may lead, in turn, to unsuccessful validation.

If a code is used in a correct way, the quality of input data will determine the final result. Input data are usually provided either from measurements or from databases. Data acquisition is a difficult, expensive and time consuming process. As far as the whole building HAM simulations are concerned, no complete set of publicly available input data exists at the moment. The situation is much better concerning the building energy simulation programs, where the validation procedure is available (see the BESTEST). For the whole building 'HAM' measurements, there is an interesting alternative that introduces ‘PASSYS[2] cells’ again, (Rode et.al., 2002b). This alternative seems promising, especially when it was shown for energy simulation programs that the ‘PASSYS’ cell facility provides data that can be easily used for the code validation (Jensen, 1993).

In situations where input data are missing, they must be either guessed or designed, and their final adjustment is usually a result of the ‘run-compare-change-run’ process (run simulation, compare results with measurements, change the input, run simulations again). This process automatically excludes the ‘blind’ validation, i.e. validation where the measured data are not available. In addition, the sensitivity analyses should be included in the validation report, showing to what extent the designed value can influence the final result. If the missing parameter is highly correlated to some other (important parameters), the validation may not be possible.

For the empirical validation of the HAM-Tools ‘Whole building’ model, measurements of temperature and relative humidity of a cold ventilated attic space in real operating conditions were selected. The “cold attic” represents an attic with a thermally well insulated floor structure. The insulation thickness varies between 220-500 mm in Sweden (Energimyndigheten, 2001). Thus, the heat input (or the heat loss) from the dwelling/office below the attic is kept to minimum and the attic remains cold throughout the winter, with the temperature close to the outdoors one.

Over the years of such practice, cold attics have encountered problems of mold growth due to certain temperature and relative humidity range combinations (they usually occur in the autumn) and due to the long duration of such periods. Several investigations have been done on this topic looking for the cause and the remedy to the problem.

One of such research projects was organized by the Swedish National Testing and Research Institute, during 1994-1995. The aim of the project was to investigate the influence of the ventilation rates and the moisture buffering effect of the insulation on the indoor climate of the cold attic, by measurements taken on the spot. Because of that, the whole attic area was divided in six sections, Figure 5.4, and measurements were performed in each of them.

The data obtained in this project have been used previously for code validation (Samuelson, 1995), and here for the HAM-Tools attic model validation. The comparison between measurements and calculations is presented in a way which was also used in the cited reference:

- Variations in time,
- Monthly mean values and
- Duration curves.

[2] PASSYS cell test facility enables the monitoring of the performance of representatively sized building systems and/or full scale components in real outdoor climate with a controlled or measurable indoor environment. The facility originates from the European PASSYS Project (1987-1992). One of the main aims of the project was the evaluation of both steady-state and dynamic performance characteristics of passive solar components. Since then, the cells were used for a variety of other applications where the use of a test cell would provide information not readily available by other, more standard tests.

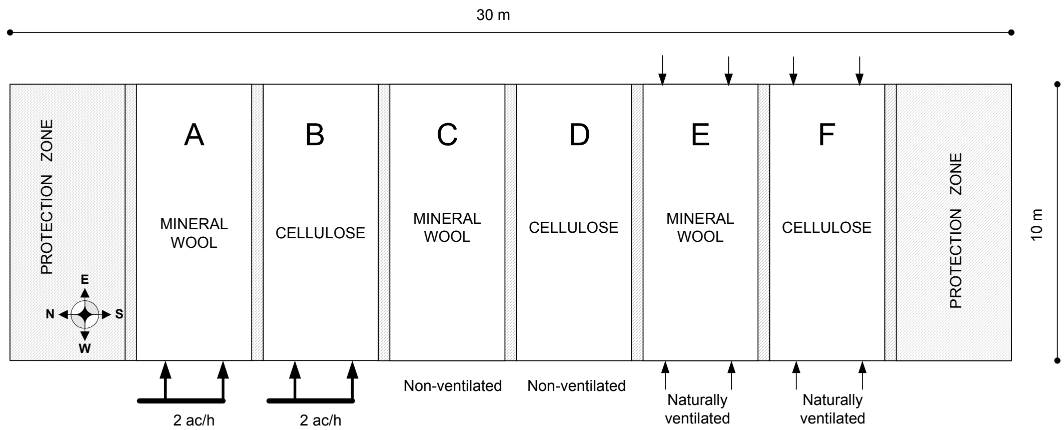

Figure 5.4 Attic sections.

Comparison by the first method 'Variations in time' is illustrated in Figures 5.5 and 5.6. Figures show calculated and measured climate in selected attic sections. The selection is made to show one of the cases with 'very good' agreement between calculation and measurements (Figure 5.5, section 'C'), and the one where the lowest quality of the agreement is achieved (Figure 5.6, section 'E'). The differences in relative humidities between sections are obviously depending on the ventilation regime, and the moisture buffering capacity of insulation, but the thermal climate is almost the same.

Mean values for the temperature and relative humidity in each section and during the whole simulated period are given in Figure 5.7. This Figure illustrates the second method of comparison 'Monthly mean values'.

Results for the relative humidity sorted in descending order, for sections 'C' and 'E' are given in Figures 5.8 and 5.9. These, so called 'Duration curves' show the quality of agreement and should be used in the following way (Samuleson, 1995): if the curve is horizontal or close to that, the climate is considered stable. On the other hand, the steeper the curve, the bigger variations in climate are taking place. If curves have the same slope but are on different levels, it implies that one section is a little colder or warmer than the other one.

Beside presented examples, the parametric sensitivity analyses have been performed and necessary adjustments for the lacking input data have been fully documented. The code has shown a high degree of reliability, both in a qualitative and in a quantitative way. The outlines of this validation are presented in **Paper V**, and in the complete form in Sasic (2003).

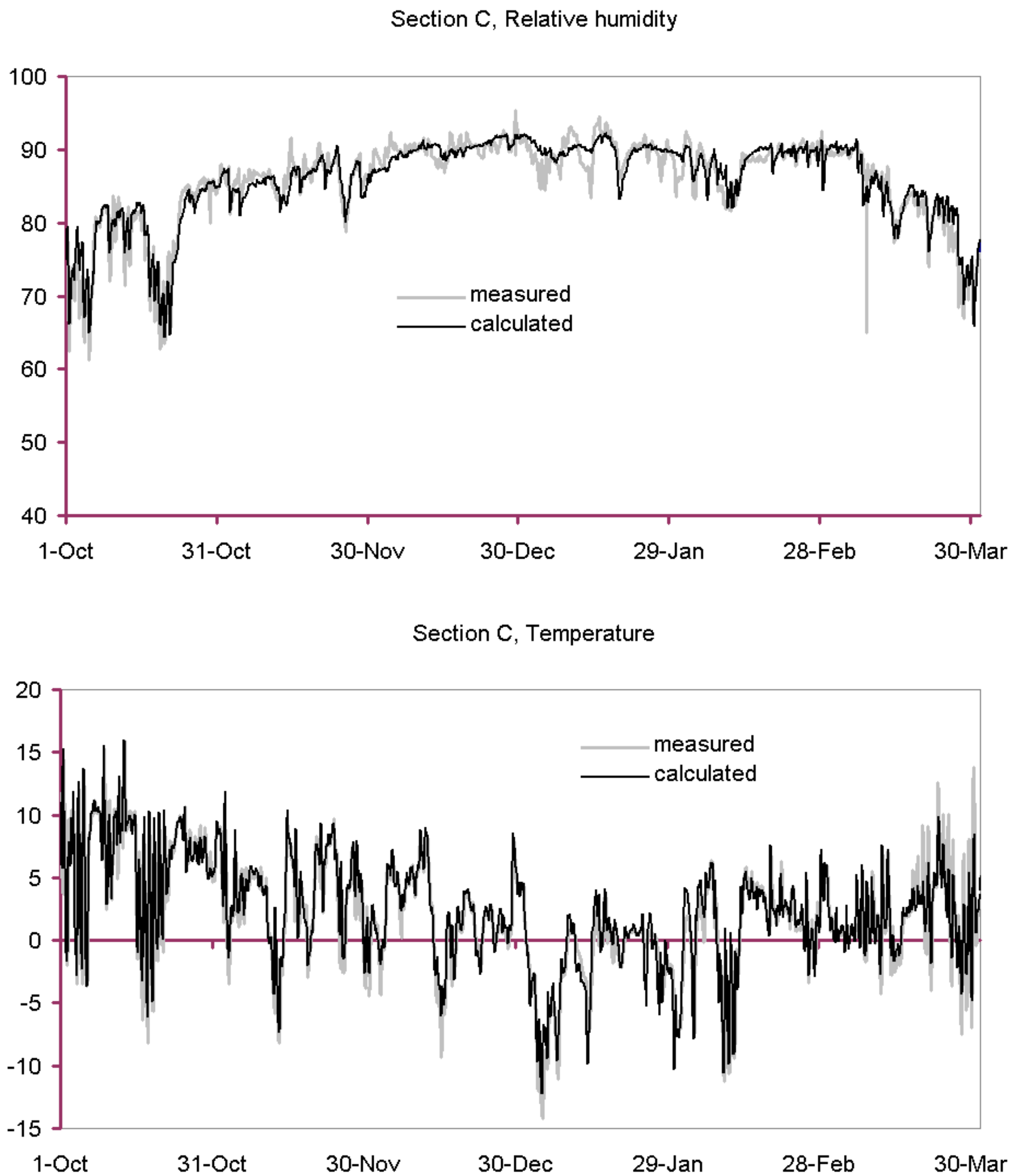

Figure 5.5 Results for section 'C'. Calculated temperature and relative humidity versus measured ones.

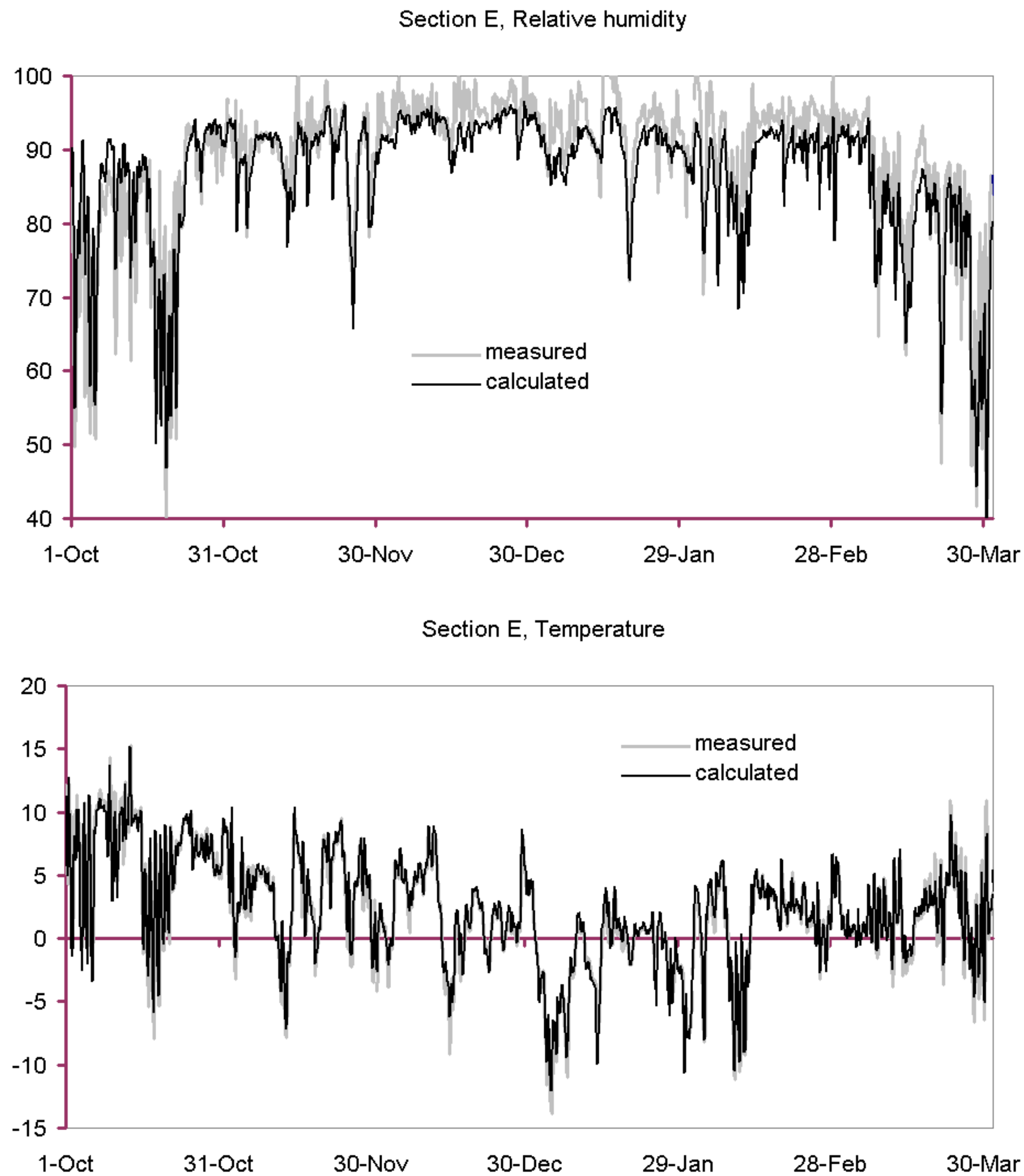

Figure 5.6 Results for section 'E'. Calculated temperature and relative humidity versus measured ones.

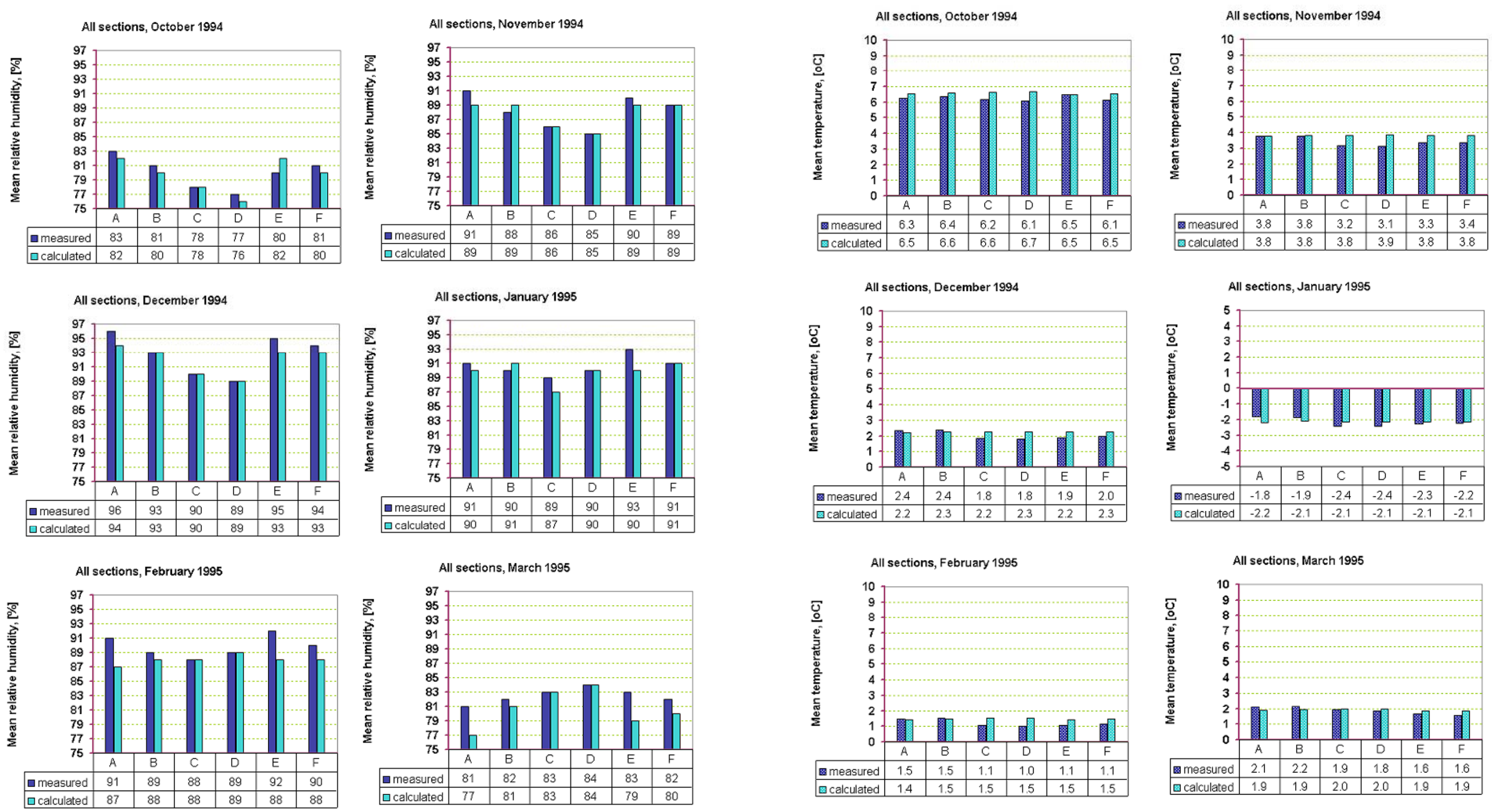

Figure 5.7 Calculated and measured mean values of relative humidity and temperature. Results are given for each section, during the whole simulation period.

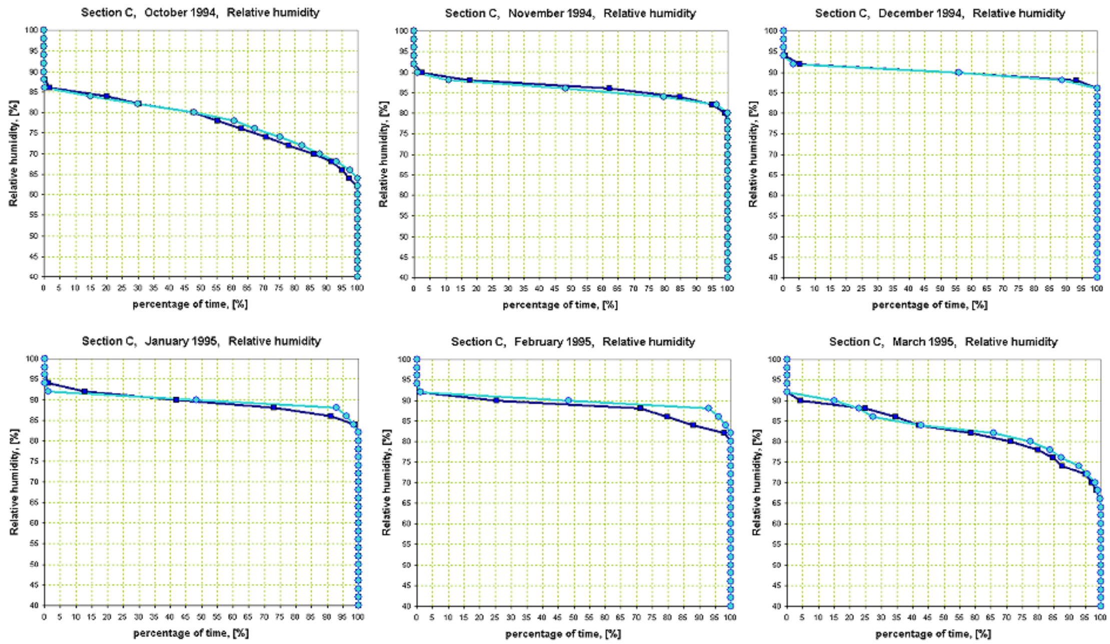

Figure 5.8 Duration curves for the relative humidity in sections 'C'. Measured data are denoted with the dark line, and the calculated with the gray line.

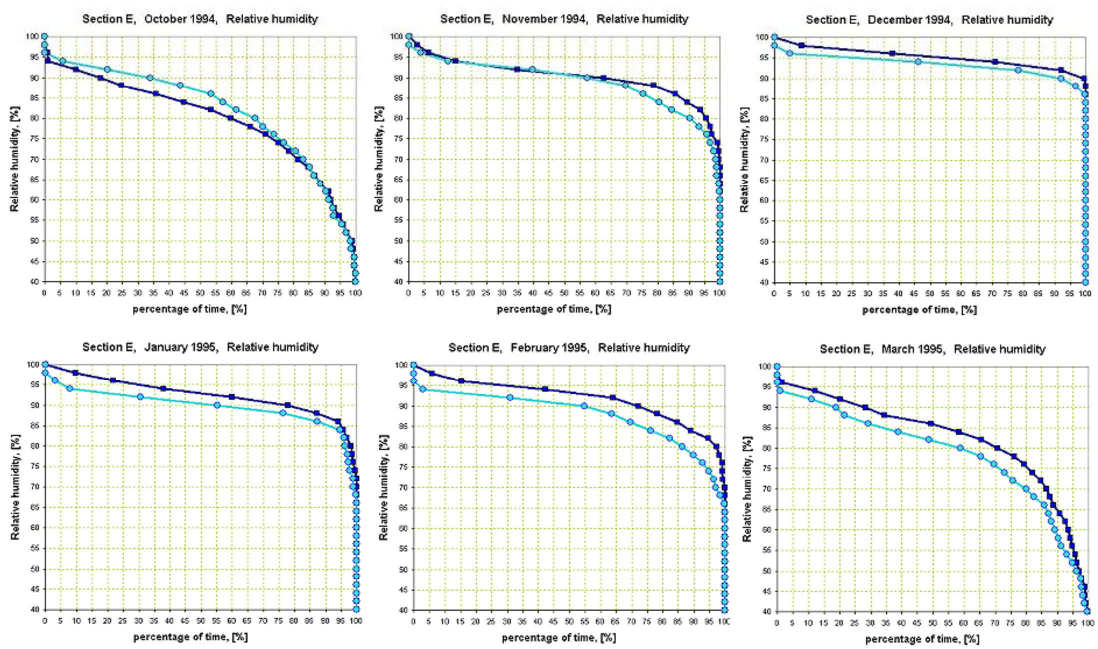

Figure 5.9 Duration curves for the relative humidity in sections 'E'. Measured data are denoted with the dark line, and the calculated with the gray line.

6. CONCLUSIONS

The work presented can be summarized in the following outlines:

- A simulation tool for the whole building heat, air and moisture response has been presented. The tool provides a numerical solution of the hygro-thermal states inside the building envelope and in internal air zones, as a result of the interaction with specified external climate data, applied HVAC systems and occupancy.

- The tool is designed as a modular structure of standard building elements; five categories have been defined:

Constructions	(external / internal walls and windows)
Zones	(air volume of the room)
Systems	(HVAC systems)
Helpers	(handling of weather data)
Gains	(internal heat and moisture gains)

  Each element represents a separate calculation procedure - the ‘tool’. Using the graphical programming language Simulink, tools are designed as graphical block diagrams and placed in the ‘library’ file called ‘HAM-Tools’

- Heat, air and moisture transport processes in building construction elements are simplified to one-dimensional problems.

- Heat, air and moisture transport processes in building air zones are simplified to the one-air node, representing well-mixed air.

- By using the system of seven well defined data signals, tools may be combined in a more complex calculating procedure, leading to a prototype of a building as a system. Thus, the whole program represents an integrated simulation tool.

- Such structured interface is mandatory only for the highest level of programming, e.g. the level where completed tools like Constructions, Zones, etc. can be combined. The main purpose of this interface is to allow the independent tool development, so that they can be exchanged between different partners.

- The numerical model for the multi-layered wall (‘Construction’ block) has been validated by comparing simulated results with an analytical solution and with solutions obtained from different codes (inter-model comparison). The model for the whole building, which is composed from the standard tools like ‘Construction’, ‘Zone’ and ‘System’ blocks has been validated against measurements. In all cases, the tool has shown a high level of reliability.

- Some selected examples of the code application show its possibility to encounter non-linear HAM effects, such as the occurrence of interstitial condensation, rapid wetting or air-driven moisture transport. The model for the whole building shows the ability of the code to evaluate the indoor climate regarding the interaction between the building envelope, external climate data and occupancy.

- The tool is an open source, available to anyone who has an interest either to use it or to participate in its development. Regarding the latter interest, moderate to advanced knowledge in building physics is required.

7. FURTHER DEVELOPMENT

Already from the beginning, the 'HAM-Tools' has been developed as an open and publicly available source, so that any researcher and student may use, expand, and develop the contents of the library. One of additional features of the library is that the heat, air and moisture calculations can be easily decoupled, so the library can be split into 'H', 'A' and 'M' tools. The other way is also possible, i.e. to upgrade the calculations with additional process. Here are some examples:

1. 'Fast tool for predictions of the climate inside a car passenger compartment' (Lundin, E. 2003).

This calculation tool gives the assessment for the overall energy requirements for a car passenger compartment. The work focused on the air temperature in the upper parts of the compartment and the surface temperature of the instrument panel during the longer exposure to the direct solar radiation. The functionality of the car air-conditioning system was also concerned. Calculations were validated with measurements from Volvo Car Corporation climate wind tunnel, and satisfactory agreement was achieved. The tool is developed mainly to serve as an additional, fast calculation tool with some others based on CFD calculations. The 'H' tool has been used as the base for the tool development.

2. A numerical model for dynamic simulations of volatile organic compounds in indoor air. (Karlsson H. 2004)

The concentration of harmful volatile organic compounds (VOC) in indoor air has recently become an issue of consideration among researchers. It has been proved that building interior finishes can release and store these substances under longer periods, decreasing (sometimes even latently) the quality of indoor environment. Using the Simulink modeling environment, a calculation tool 'VOC-Tools' is developed for assessing the VOC concentration in indoor air. This tool treats storage and releasing of selected VOCs from building materials, furniture, appliances, inhabitants, ventilation system, etc., governed by convection, sorption and diffusion processes. 'HAM-Tools' has been used as a pattern for the tool development. There is a plan to combine these tools in the future, in order to assess the influence of the HAM states in building and building components on the VOC release.

Further applications and development of HAM-Tools is determined by the interest of future users and their contributions. Hopefully, it will be done in the following areas:

- Development of the 'Systems', 'Gains' and 'Helpers' libraries, with more detailed designed blocks (control systems, more cases, indoor climate classes)

- Extending the interface to allow the coupling with other codes that include non-existing features like 2D and 3D effects.

- More validation tests. The first possibility is seen through the engagement in the Annex 41, where different exercises regarding the whole building HAM simulations will be enclosed.

REFERENCES

Augenbroe, G. 2001. Building simulation trends going into the new millennium. Proceedings of the 7th International Building Performance Simulation (IBPSA) Conference. Rio de Janeiro, Brazil.

ASHRAE 2002. A thermal and moisture transport database for common building and insulating materials. Report RP-1018. American Society of Heating, Refrigerating and Air-Conditioning Engineers, Inc.

Bergsten, B. Energy calculation programs for buildings. Comparison from the functionality and user aspects. In Swedish. Effektiv. Report 2001:03.

Judkoff, R., Neymark, J. 1995. International Energy Agency. Building Energy Simulation Test **(BESTEST)** and Diagnostic Method. National Renewable Energy Laboratory. Golden. Colorado.

Blocken, B., Desadeleer, W., Carmeliet, J. 2003a. Numerical study of façade disfigurement by driving rain. Research in Building Physics. Proceedings of the 2nd International Conference in Building Physics. Antwerpen. Belgium.

Blocken, B., Roels, S., Carmeliet, J. 2003a. A numerical study of wind nuisance of a high-rise building group. Research in Building Physics. Proceedings of the 2nd International Conference in Building Physics. Antwerpen. Belgium.

Broken, H. 1998. Moisture transport in brick masonry: the grey area between bricks. Doctoral thesis. Eindhoven University of Technology. The Netherlands.

Carmelite, J., Roels, S. 2002. Determination of the moisture capacity of porous building materials. Journal of Thermal Envelopes and Building Science, Vol. 25 – January.

CEN/TC 89 WI 29.3. Hygrothermal performance of building components and building elements – Assessment of moisture transfer by numerical simulation.. Draft.

Claesson, J., Hagentoft, C-E., Sällfors, G. 2003. Analyzes of highly non-linear, coupled moisture and heat flow in bentonite based on radial, steady-state solutions. Report SKI. Department of Building Physics, Chalmers University of Technology, Gothenburg, Sweden.

Energimyndigheten, 2001. Actual small houses in Sweden. In Swedish. Eskilstuna, Sweden.

Fletcher, C.A.J. 1987. Computational techniques for fluid dynamics 2. Specific techniques for different flow categories. Springer-Verlag.

Galbraith, G.H., Kelly, D.J., McLean, R.C. 2003 Alternative methods for measuring moisture transfer coefficients of building materials. Research in Building Physics. Proceedings of the 2nd International Conference on Building Physics, Antwerpen, Belgium.

Grünewald, J., Plagge, R., Bomberg, M. 2001 Advantages and disadvantages of lumped-parameter or phase-dividing functions. International Conference on Building Envelope Systems and Technologies, ICBEST-2001, Ottawa, Canada.

Hagentoft, C-E. 2002a. HAMSTAD WP2 Modelling, Version 4. Report R-02:9. Department of Building Physics, Chalmers University of Technology, Gothenburg, Sweden.

Hagentoft, C-E. 2002b. Final report: Methodology of HAM-Modelling. Report R-02:8. Department of Building Physics, Chalmers University of Technology, Gothenburg, Sweden.

Hagentoft, C-E., **Sasic Kalagasidis, A., Adl-Zarrabi, B. Roels, S., Carmeliet, J., Hens, H., Grunewald, J., Funk, M., Becker, R., Shamir, D., Adan, O., Brocken, H., Kumaran, K., Djebbar, R. 2004**. Assessment Method of Numerical Prediction Models for Combined Heat, Air and Moisture Transfer in Building Components: Benchmarks for One-dimensional Cases. Journal of Thermal Envelope and Building Science, Vol. To be published.

IEA-EXCO, Annex 41. 2003. Whole building heat, air and moisture response (MOIST-ENG). International Energy Agency (IEA) – (EXCO) Energy Conservation in Buildings and Community Systems.

Janssens, A. 1998. Reliable control of interstitial condensation in lightweight roof systems. Calculation and assessment methods. Doctoral thesis. The Catholic University of Leuven, Belgium.

Jensen, S. Ø. 1993. Empirical whole model validation. Case study: the PASSYS reference wall. Proceedings of the 3rd International Building Performance Simulation (IBPSA) Conference. Adelaide. Australia.

Karlsson, H. 2004. The numerical model for dynamical simulations of organic volatiles in indoor climate. Master thesis. Report E-04:01. Department of Building Technology, Chalmers University of Technology, Gothenburg, Sweden.

Klemm, K., Jablonski, M. 2003. Effect of windbreak on the wind flow in a small existing urban structure. Research in Building Physics. Proceedings of the 2nd International Conference in Building Physics. Antwerpen. Belgium.

Kumaran, K. 1996. IAE Annex 24, Final Report, Volume 3, Material properties. K.U.Leuven, Belgium: Laboratorium Bouwfysica, Departement Burgerlijke Bouwkunde.

Lundin, E. 2003. Fast tool for predictioins of the climate inside a car passenger compartment. Master thesis. Report E-03:04. Department of Building Technology, Chalmers University of Technology, Gothenburg, Sweden.

Maliska, C.R. 2001. Issues on the integration of CFD to building simulation tools. Proceedings of the 7th International Building Performance Simulation (IBPSA) Conference. Rio de Janeiro, Brazil.

Nilsson, P.E. 2003. Achieving the Desired Indoor Climate. Energy efficiency aspects of system design. Studentlitteratur. Lund. Sweden.

Rode, C., Gudum, C., Weitzmann, P., Peuhkuri, R., Nielsen, T. R., Sasic Kalagasidis, A., Hagentoft, C-E. 2002a. International Building Physics Toolbox, General report. R-02:4. Gothenburg: Chalmers University of Technology, Department of Building Physics. Also available on **www.ibpt.org**.

Rode, C., Mitamura, T., Schultz, J., Padfield, T. 2002b. Test Cell Measurements of Moisture Buffer Effects. Proceedings of the 6th Symposium Building Physics in the Nordic Countries. Trondheim. Norway.

Roels, S. 2000. Modelling unsaturated moisture transport in heterogeneous limestone. Doctoral thesis. The Catholic University of Leuven, Belgium.

Samuelson, I. 1995 Moisture balance in the cold attics. The importance of Ventilation and Choice of Insulation Materials. In Swedish. SP rapport 1995:68. Borås, Swedish National Testing and Research Institute.

Sanders, C. 1996. IAE Annex 24, Final Report, Volume 2, Environmental conditions. K.U.Leuven, Belgium: Laboratorium Bouwfysica, Departement Burgerlijke Bouwkunde.

Sasic Kalagasidis, A. 2002. HAM-Tools, International Building Physics Toolbox, Block documentation. Report R-02:6. Department of Building Physics, Chalmers University of Technology, Gothenburg, Sweden. Also available for free downloading on www.ibpt.org.

Sasic Kalagasidis, A. 2003. The whole model validation for HAM-Tools. Case study: hygro-thermal conditions in the cold attic under different ventilation regimes and different insulating materials. Report R:03-6. Department of Building Technology, Chalmers University of Technology, Gothenburg, Sweden. Also available for free downloading on www.ibpt.org.

Serkitjis, M., Sasic Kalagasidis, A. 2004. Practical consequences of the altered thermal performance of the attic loose-fill insulation due to induced air movement. Accepted for the International Thermal Science Seminar, ITSS II, Bled, Slovenia.

Segerholm, I. 2004. Nonisothermal moisture transport properties in wood evaluated from experiments. Submitted to Wood science.

TN AIVC 44. 1998. Numerical Data for Air Infiltration & Natural Ventilation Calculations. Air Infiltration and Ventilation Center. International Energy Agency.

Wang, J. 2003. Heat and mass transfer in built structures – numerical analyses. Doctoral thesis. Chalmers University of Technology, Gothenburg, Sweden.

de Wit, M. 2000. A simulation model for the thermal and hygric performance of a building. Technical University Eindhoven, the Netherlands.

Internet sites, computational codes and databases

BES (Building Energy Software) Tools Directory. www.eere.energy.gov/buildings/tools_directory/

ECBCS Energy Conservation in Buildings & Community Systems Programme. International Energy Agency. www.ecbcs.org/Annexes.htm

ESP-r. University of Strathclyde. Glasgow, Scotland.

Fluent. 2004. CFD package. AAVID Thermal Technologies. UK.

IBPT. International Building Physics Toolbox. www.ibpt.org.

IDA. Indoor Climate and Energy. Sweden.

METEONORM. Global Meteorological Database for Solar Energy and Applied Climatology. Version 4.0. Software and Data on CD-ROM. Meteotest, Switzerland.

MathWorks. Simulink and MatLab software packages. Available from www.mathworks.com

SPARK. Simulation Problem Analysis and Research Kernel. Lawrence Berkeley National Laboratory. Berkeley. California.

TRNSYS. Transient System Simulation Program. Solar Energy Laboratory, University of Wisconsin. Madison. Wisconsin.